Journal of Catalysis 302 (2013) 67–82

Contents lists available at SciVerse ScienceDirect

Journal of Catalysis

journal homepage: www.elsevier.com/locate/jcat

Reaction intermediates of ethanol electro-oxidation on platinum investigated by SFG spectroscopy

Janaina F. Gomes [a], Kleber Bergamaski [b,1], Melissa F.S. Pinto [b,2], Paulo B. Miranda [b,*]

[a] Instituto de Química de São Carlos, Universidade de São Paulo, C.P. 780, São Carlos, SP 13560-970, Brazil
[b] Instituto de Física de São Carlos, Universidade de São Paulo, C.P. 369, São Carlos, SP 13560-970, Brazil

ARTICLE INFO

Article history:
Received 16 November 2012
Revised 25 February 2013
Accepted 27 February 2013
Available online 9 April 2013

Keywords:
SFG spectroscopy
DFT
Electro-oxidation
Ethanol
Platinum
Adsorbed intermediates

ABSTRACT

Although electrochemical oxidation of simple organic molecules on metal catalysts is the basic ingredient of fuel cells, which have great technological potential as a renewable source of electrical energy, the detailed reaction mechanisms are in most cases not completely understood. Here, we investigate the ethanol–platinum interface in acidic aqueous solution using infrared–visible sum frequency generation (SFG) spectroscopy and theoretical calculations of vibrational spectra in order to identify the intermediates present during the electro-oxidation of ethanol. The complex vibrational spectrum in the fingerprint region imply on the coexistence of several adsorbates. Based on spectra in ultra-high-vacuum (UHV) and electrochemical environment from the literature and our density functional theory (DFT) calculations of vibrational spectra, new adsorbed intermediates, never before observed with conventional infrared (IR) spectroscopy, are proposed here: η^2-acetaldehyde, η^2-acetyl, ethylidyne, monodentate acetate, methoxy, tertiary methanol derivative, COH residue, η^2-formaldehyde, mono and bidentate formate, CH_3 and CH_2 residues. In addition, we present new evidences for an ethoxy intermediate, a secondary ethanol derivative and an acetyl species, and we confirm the presence of previously observed adsorbates: a tertiary ethanol derivative, bidentate acetate, and CO_{ad}. These results indicate that the platinum surface is much more reactive, and the reaction mechanism for ethanol electro-oxidation is considerably more complex than previously considered. This might be also true for many other molecule-catalyst systems.

1. Introduction

Electrochemical oxidation of simple organic molecules on metal catalysts is at the heart of fuel cells, which have great technological potential as a renewable source of electrical energy. Direct alcohol fuel cells, especially those using ethanol as a fuel, are becoming a very attractive alternative energy source for fossil fuels due to several advantages: (i) easier and safer transportation and storage of liquid fuels when compared to gases; (ii) the theoretical mass energy density of alcohols such as methanol and ethanol is high and comparable to gasoline [1,2], and the thermodynamic efficiency of fuel cells is much higher than internal combustion engines; (iii) ethanol can be mass-produced by renewable sources, is less pollutant than fossil fuels, and can share the available gasoline distribution infrastructure [3]; (iv) ethanol is a good candidate for polymeric electrolyte membrane fuel cell (PEMFC) due to its low permeability through polymeric membranes and also for leaving less toxic by-products [2]. However, before they become widely available, a few technological issues need to be overcome. In regard to the electrochemical reaction, the main problems that need to be addressed are the high overpotential for the oxidation reaction due to the presence of poisoning adsorbed intermediates at low potentials and the formation of partially oxidized products. The solution to them necessarily demands a thorough understanding of the detailed reaction mechanisms, which are in most cases not completely understood. Therefore, the possible application of ethanol as a fuel for direct alcohol fuel cells continues to motivate research aimed at developing a mechanistic understanding of the electro-oxidation of ethanol.

Fundamental studies of ethanol electro-oxidation in acid media were mostly performed on platinum and its alloys [4–8]. Among various Pt-based binary catalysts, Pt—Sn has been reported as the most effective for the electro-oxidation of ethanol [4,9]. Palladium has been studied less actively in acid media due its relatively low performance. On the other hand, in alkaline media, palladium appears to be quite active for ethanol oxidation [10]. Palladium-based alloys in alkaline media have also received significant attention [11], even though the ethanol oxidation on a pure palladium electrode has not yet been fully understood.

* Corresponding author.
E-mail address: miranda@ifsc.usp.br (P.B. Miranda).
[1] Current address: Departamento de Química, Universidade Federal de Sergipe, Rod. Marechal Randon, s/n, São Cristóvão, SE 49100-000, Brazil.
[2] Current address: Departamento de Física – ICEB, Universidade Federal de Ouro Preto, Campus Morro do Cruzeiro, Ouro Preto, MG 35400-000, Brazil.

0021-9517/$ - see front matter © 2013 Elsevier Inc. All rights reserved.
http://dx.doi.org/10.1016/j.jcat.2013.02.024

Concerning the ethanol oxidation on Pt electrodes, although it is well-known that it follows parallel reaction pathways leading to acetaldehyde, acetic acid and CO_2 [9,12–15], the mechanism of this reaction remains unclear. There is not yet a consensus concerning the adsorbed intermediates that lead to the formation of these products. From Differential Electrochemical Mass Spectrometry (DEMS) investigations, it was concluded that the CO_2 can originate from either the alcohol or the methyl groups of the ethanol [12,16]. However, the available data related to the dissociation of the C—C bond are contradictory. On one hand, Willsau and Heitbaum [12] suggested that the adsorbed intermediate contains the intact C—C bond of ethanol. On the other hand, Bittinscattaneo et al. [16] proposed that the ethanol adsorbs mainly dissociatively in form of one carbon atom species. In 1994, the Fourier Transform Infrared (FTIR) and DEMS results published by Iwasita and Pastor [17] showed that the presence of an acetyl residue could not be discarded. This partially agrees with the idea of Willsau and Heitbaum [12]. Nevertheless, it was demonstrated that the acetyl was not the only adsorbed species formed [17]. Adsorbed CO was clearly evident. In addition, it was proposed that the secondary alcohol derivative (Pt—CHOH—CH_3) could be the precursor for the formation of the adsorbed CO via an acetyl species. However, no direct evidence of the ν(C—OH) band of a secondary alcohol [18] was observed in that work [17]. Based on Electrochemically Modulated Infrared Reflectance Spectroscopy (EMIRS), different models for the adsorbed species were discussed, including the adsorption of an ethoxy species [19]. Acetaldehyde [20], acetic acid [21], and acetyl [22] were also proposed as adsorbed intermediates of ethanol oxidation.

Undoubtedly, the studies described above have contributed enormously to the elucidation of the complex mechanism of the ethanol oxidation on platinum. However, it is important to emphasize that in all these studies, the electro-oxidation of ethanol was investigated by linear spectroscopic techniques. The disadvantage of using this kind of spectroscopic probe is that it is impossible to completely discriminate features from adsorbates and contributions from bulk species. Eliminating the contribution from the bulk is critical when the adsorbed intermediates and the bulk products contain the same functional groups, as for the partially oxidized products acetaldehyde and acetic acid. In such cases, it is difficult to differentiate between bulk and adsorbed species and hence difficult to make unambiguous identifications of adsorbed intermediates. Sum-Frequency Generation (SFG) spectroscopy can be used as a powerful tool to obtain vibrational spectra of adsorbed species without contribution from the bulk [23,24]. Since SFG is a second-order non-linear optical process that occurs only at media where the inversion symmetry is broken, it is allowed only at the interface between two centrosymmetric materials, making it possible to detect adsorbed species without any contribution from the bulk. Because of this major advantage, SFG spectroscopy has already been used by several groups to investigate the electrochemical interface, notably on Pt electrodes. However, these studies are usually limited to vibrations with high dipole moment and polarizability derivatives, such as adsorbed CO or CN [25–32]. One exception is the formation of Pt—OH detected by SFG spectroscopy [33]. Very recently, Kutz et al. [34] have investigated ethanol electrooxidation on polycrystalline Pt using SFG spectroscopy. They only detect adsorbed CO and acetate ions (and (bi)sulfate ions, for the case of sulfuric acid supporting electrolyte). Furthermore, using ^{13}C-labeled ethanol, they demonstrate the cleavage of the C—C bond upon electrochemical adsorption. It should be also mentioned the very recent SFG study by Braunschweig et al. [35] of acetic acid electrochemical adsorption onto Pt and Au electrodes, where they also found adsorbed acetate ions, as in Ref. [34]. Although these studies have further advanced our understanding of the electro-oxidation of simple molecules on Pt electrodes, the detection and identification of other species, including those previously suggested by IR spectroscopy, is still lacking.

In this work, we will present the first SFG spectra of ethanol in acidic medium at a polycrystalline platinum surface over a wide spectral range (1000–3300 cm^{-1}). The main purpose of the present work is to identify adsorbed intermediates of the ethanol oxidation on Pt using SFG spectroscopy and DFT calculations of their vibrational spectra. In contrast to previous SFG experiments, our results indicate the coexistence of several adsorbates. In addition to presenting new evidences for previously suggested intermediates and confirming the presence of adsorbates already observed by IR and SFG spectroscopies, we identify new adsorbed intermediates. As an aid to the reader, Fig. 9 (at the end of Section 3.4) displays the structure of potential adsorbates that will be discussed in the text.

2. Methodology

2.1. Experimental section

Similar to previous work [25,28], the SFG experiments were performed in a three electrode spectro-electrochemical cell with an IR and visible transparent 2 mm CaF_2 window attached to the top of the cell. The working electrode was a polished polycrystalline platinum disk 12 mm in diameter. A platinized platinum wire and a reversible hydrogen electrode were used as the counter and reference electrodes, respectively. A movable piston supports the working electrode. A platinum wire connected to the working electrode passes through the piston and keeps the electric contact. Before each experiment, the working electrode was annealed in a H_2 flame for approximately 15 min, cooled to room temperature in an inert N_2 atmosphere and then protected with a drop of water to prevent contamination before being transferred to the spectro-electrochemical cell. The working electrode was introduced at open circuit potential to the spectro-electrochemical cell containing 0.1 M ethanol and 0.5 M $HClO_4$ and subsequently polarized at 0.05 V. SFG spectra were taken in the region between 1000 cm^{-1} and 3300 cm^{-1}, at potentials increasing from 0.05 V to 1.1 V vs. RHE (0.05 V steps), waiting about 1 min after setting each potential. The complete range of wavenumbers was scanned in four different experiments. During the acquisition of the SFG spectra, the working electrode was pressed against the CaF_2 window to obtain a thin liquid film in order to minimize the absorption of the infrared beam by the electrolytic solution. The maximum attenuation of the reflected IR beam in the spectral range from 1000 to 2100 cm^{-1} occurs at 1650 cm^{-1}, and it varied from 60% to 90% (crossing the liquid film twice), which corresponds to a single pass attenuation of ~37–68%. The SFG spectra were not corrected for this effect. From these measurements, the thickness of the thin electrolyte layer is estimated to be 2.65 ± 0.75 μm. However, the stronger IR absorption of water in the OH stretch range attenuated most of the IR energy, making the SFG spectra unreliable above 3200 cm^{-1} (or between 2350 cm^{-1} and 2700 cm^{-1}, for experiments with deuterated water). From 1250 cm^{-1} to 1000 cm^{-1}, the IR transmittance decreases from 95% to 60% due to bulk IR absorption of the 2 mm CaF_2 window. Our results were also not corrected for this effect.

The SFG spectrometer (Ekspla, Lithuania) consists of a flash-lamp-pumped Nd^{+3}:YAG laser that generates 25 ps pulses at 1064 nm with a repetition rate of 20 Hz. A 532 nm beam is produced by second harmonic generation (SHG) and a tunable IR beam (2.5–10 μm, bandwidth ~3 cm^{-1}) is produced by an optical parametric generator/amplifier (OPG/OPA) followed by a difference-frequency generation (DFG) stage. Before the SFG experiments, the alignment of beams (temporal and spatial overlap of beams

on the sample and SFG signal detection) was optimized on a reference sample of intense nonresonant signal (quartz or ZnS), which was then replaced by the sample of interest. The p-polarized 532 nm and IR beams overlapped temporally and spatially on the sample with spot sizes and angles of incidence of ~1.0 mm and ~0.5 mm, and 61° and 55°, respectively. The p-polarized SFG signal of the platinum–solution interface was normalized to the IR pulse energy, which was monitored before reaching the sample and recorded simultaneously with data acquisition. Each data point in the SFG spectrum is an average of 125 shots. The energies of visible and IR pulses were about 40 μJ and 50 μJ, respectively.

2.2. Theoretical section

We have used the density functional theory (DFT) approach to perform calculations of vibrational spectra to support peak assignments of the experimental SFG spectra. For that purpose, we have compared the calculated vibrational spectra of several potential intermediates adsorbed on a Pt cluster to the observed SFG resonances. This demanded a high accuracy in the calculation of vibrational frequencies, since the SFG peaks were quite closely spaced (~20–50 cm^{-1}). The Pt cluster was constructed using the crystallographic data reported by Waseda et al. [36] for FCC platinum with space group Fm-3m, with cell parameters $a = b = c = 392.42$ pm and $\alpha = \beta = \gamma = 90°$. In this configuration, the distance between the Pt atoms is 277.5 pm [36]. The cluster was arranged to model the Pt(1 1 1) surface, with the first layer consisting of ten platinum atoms and the second layer having six platinum atoms, as shown in Fig. 1. The third layer was discarded because it has minimal influence on properties under study, as well as to minimize the computational effort in electronic structure calculations. The platinum cluster was maintained fixed and we carried out fully relaxed geometry optimizations of the ethanol-derived adsorbates, which were attached to the central Pt atom of the first layer. Calculations also showed that, within the extent and arrangement of our Pt(1 1 1) model, the position of a second bond for bidentate adsorbate has minimal effect on spectroscopic assignments.

The potential adsorbates investigated were the following: CO, secondary and tertiary ethanol derivative, acetyl, bidentate acetate, ethoxy and η^2-acetaldehyde. The interactions between these derivatives of ethanol and the Pt(1 1 1) model surface have been studied using density functional theory (DFT) approach, with the hybrid functional B3LYP associated with effective core potential (ECP) type basis set [37], using the GAUSSIAN 03 program [38]. In the B3LYP hybrid functional scheme, the nonlocal Hartree–Fock (HF) approach is mixed into the energy functional of the generalized gradient approximation (GGA), in which are included three parameters of Becke [39–41] for exchange energy estimation and the Lee–Yang–Parr correlation energy [42]. The Lan2DZ basis includes Dunning–Huzinaga full double zeta (DZ) basis functions for the first row and Los Alamos effective core potentials (ECPs) for heavy elements. This basis was chosen for this study because it incorporates relativistic effects for Pt (and other heavy metals), thus describing more efficiently their properties, and it is also compatible with the elements of ethanol derivatives (H, C, O). In addition, reports in the literature on platinum complexes using B3LYP/LanL2DZ level showed that it is able to reproduce with satisfactory agreement spectroscopic experimental data [43–46].

Infrared and Raman spectra calculations were carried out for all simulated adsorbates, since the SFG selection rules require that the vibrational modes must be active in both spectra. Despite the broad range of calculated spectra (up to 3500 cm^{-1}), we will discuss only the range from 1000 to 1500 cm^{-1}, which is the most prominent in the experimental spectra and is the most sensitive to molecular structure (vibrational fingerprint region).

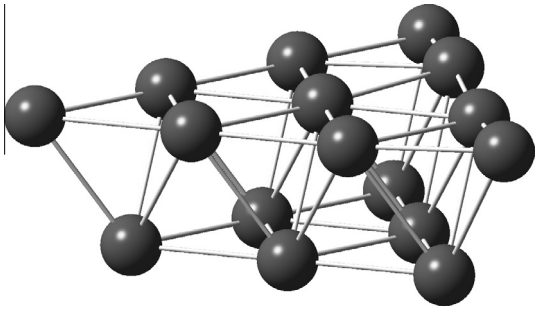

Fig. 1. Side view of the Pt(1 1 1) cluster model.

3. Results and discussion

3.1. Vibrational spectra of adsorbates

Before exploring the vibrational spectra of adsorbates of the ethanol oxidation on Pt in acidic medium, the cyclic voltammogram of the polycrystalline platinum electrode in 0.5 mol L^{-1} $HClO_4$ + 0.1 mol L^{-1} ethanol is introduced in Fig. 2. In the positive-going scan, the oxidation of ethanol begins close to 0.40–0.50 V and the current peaks at 0.90 V and 1.30 V. In the negative-going sweep, the current starts to increase at 0.90 V, reaches a maximum at 0.65 V, and then decreases to nearly zero at 0.40 V. These results are in accord with those previously observed for 0.1 mol L^{-1} ethanol over polycrystalline platinum in acidic medium [20].

Fig. 3 shows the SFG spectra (from 1000 cm^{-1} to 3300 cm^{-1}) of the 0.5 mol L^{-1} $HClO_4$ + 0.1 mol L^{-1} ethanol–Pt interface at 0.30 V (filled circles), below the onset of the first oxidation current peak. In these spectra, different features assigned to adsorbed species can be clearly observed. The most pronounced features are at 1056 cm^{-1}, 1084 cm^{-1}, 1122 cm^{-1}, 1168 cm^{-1}, 1214 cm^{-1}, 1270 cm^{-1}, 1408 cm^{-1}, 1432 cm^{-1}, and 2056 cm^{-1}. There are also three broad features, one between 1310 cm^{-1} and 1380 cm^{-1}, another between 1450 cm^{-1} and 1625 cm^{-1}, and a third around 1736 cm^{-1}. Based on spectra taken at other potentials (data shown in Fig. 5, Section 3.2), these features are most likely comprised of overlapping bands, at 1330 cm^{-1}, 1348 cm^{-1} and 1370 cm^{-1} for the first, and at 1475 cm^{-1}, 1496 cm^{-1} and 1546 cm^{-1} for the second. An overlapping peak at 1288 cm^{-1} and a weak feature at 1030 cm^{-1} can also be distinguished. The SFG spectra from 2100 cm^{-1} to 3300 cm^{-1} is relatively more complex to analyze,

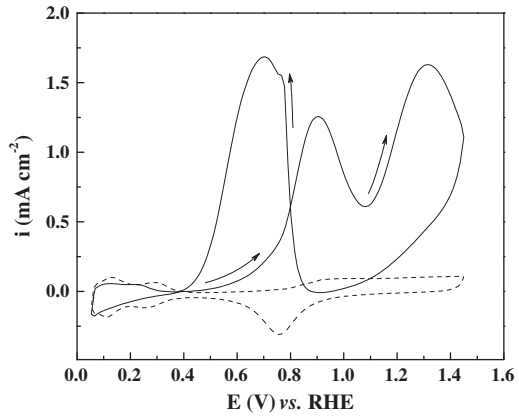

Fig. 2. Cyclic voltammogram of a polished polycrystalline platinum electrode in 0.5 mol L^{-1} $HClO_4$ (dashed line) and 0.5 mol L^{-1} $HClO_4$ + 0.1 mol L^{-1} ethanol (solid line); scan rate = 0.10 V s^{-1}.

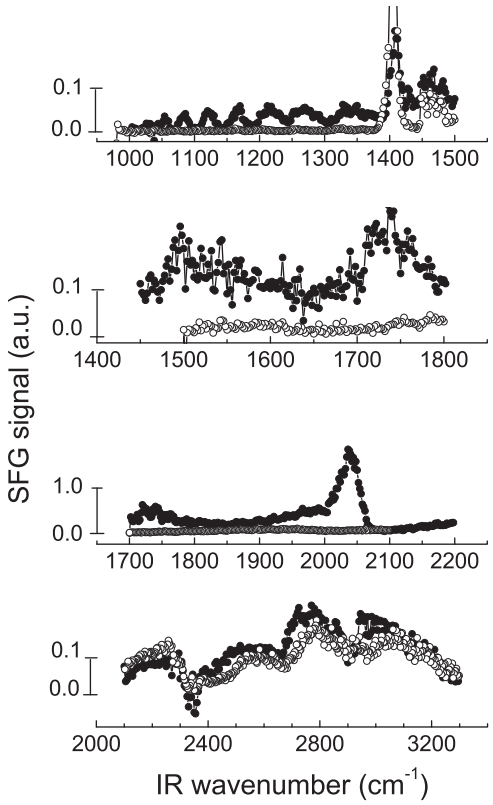

Fig. 3. SFG spectra (polarization combination PPP) of the 0.5 mol L^{-1} $HClO_4$ (empty circles) and 0.5 mol L^{-1} $HClO_4$ + 0.1 mol L^{-1} ethanol (filled circles)–polycrystalline platinum interface at 0.30 V vs. RHE.

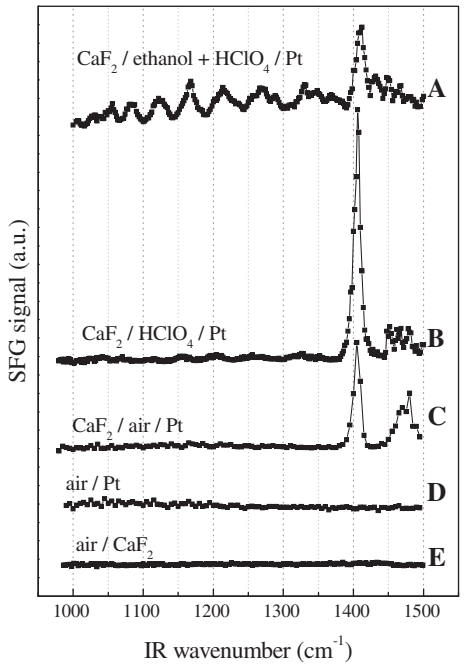

Fig. 4. SFG spectra from 1000 cm^{-1} to 1500 cm^{-1} of the following interfaces: CaF_2/0.1 mol L^{-1} ethanol + 0.5 mol L^{-1} $HClO_4$/polycrystalline platinum at 0.05 V vs. RHE (A), CaF_2/0.5 mol L^{-1} $HClO_4$/polycrystalline platinum at 0.05 V vs. RHE (B), CaF_2/air/polycrystalline platinum (C), air/polycrystalline platinum (D) and air/CaF_2 (E). The SFG spectra A, B, C, D, and E have the same *y*-axis scale, and they are offset along this axis for clarity.

since it contains weak and broad features interfering with a few narrow peaks. Among them, we clearly observe a broad band from 2650 cm^{-1} to 3200 cm^{-1}, which may be assigned to OH stretches, as will be discussed below. In order to verify that the observed bands are indeed vibrations of adsorbates on Pt derived from ethanol, we have scanned the same frequency ranges with a solution containing only the electrolyte (0.5 mol L^{-1} $HClO_4$). As seen in Fig. 3 (empty circles), most of the SFG peaks vanish, except for a prominent peak at 1408 cm^{-1}, a band between 1445 cm^{-1} and 1490 cm^{-1}, and weak bands in the region 2650–3300 cm^{-1}. Since there is no organic molecule in solution, these resonances must come from water or the electrolyte. The latter bands may be due to OH stretches of water molecules or the hydronium ion (H_3O^+) [47–50] interacting with the Pt surface by hydrogen bonding (not chemisorbed). However, the peak at 1408 cm^{-1} and the broad feature at ~1475 cm^{-1} cannot be attributed to perchlorate, water, or hydronium. We will show below that they are not due to molecular adsorbates on Pt. Therefore, except from these two spurious peaks, all other features of the SFG spectra in Fig. 3 are due to adsorbed intermediates of the electro-oxidation of ethanol on Pt. This surprising result implies that there are a lot more molecular adsorbates than previously thought, revealing a very complex reaction mechanism and making a definite assignment of all vibrational bands a formidable task. After presenting the dependence of the SFG spectra on electrochemical potential in Section 3.2 and SFG spectra with isotopically labeled reagents in Section 3.3, we will discuss in more detail a tentative assignment of these peaks in Section 3.4. For now, it suffices to say that peaks in the fingerprint range (from 1000 cm^{-1} to 1500 cm^{-1}) are due to coupled vibrations of the molecular skeleton of adsorbates, such as C—C and C—O stretches, and CH, OH, and C—C—O angular deformations [18]. A broad band at ~1700 cm^{-1} is due to the hydrogen bonded C═O stretch of adsorbates [9,15], while the intense peak at 2056 cm^{-1} is the well known C≡O stretch of linearly bonded CO on Pt [13,16,19].

Since the peaks in the frequency range from 1000 cm^{-1} to 1500 cm^{-1} are so numerous and appear to be regularly spaced, at first one could imagine that they could result from interference effects in the thin liquid film sandwiched between two reflective surfaces: the CaF_2 window and the Pt electrode. As mentioned above, this can be ruled out by the spectrum for the pure electrolyte/Pt interface shown in Fig. 3 (empty circles), where most of the resonances disappear, except for the narrow peak at 1408 cm^{-1} and a broad feature at ~1475 cm^{-1}. Additional evidence for the absence of interference effects in the thin liquid film is the comparison of the SFG spectrum taken with a 15 μm thick Teflon spacer between the window and the Pt electrode with that SFG spectrum taken without any spacer [51]. It is observed that they present similar peak positions, although with considerably reduced SFG intensities for the spectrum taken with a 15 μm thick Teflon spacer due to IR absorption by water (broad OH bending at ~1650 cm^{-1} and OH libration below 900 cm^{-1}) in this thicker electrolyte layer. If the spectra resulted from optical interference effects, the peak spacing should have been $\Delta\nu = 1/(2nd\cos\gamma)$, where γ is the beam angle with respect to the surface normal within the liquid film, n is the electrolyte refractive index, and d is the liquid layer thickness (in cm). Since the inverse relation of $\Delta\nu$ and spacer thickness is not observed, interference cannot explain the observed SFG spectra below 1500 cm^{-1}.

We will now turn to the origin of the SFG bands at 1408 cm^{-1} and ~1475 cm^{-1}. As will be shown in Section 3.2, the intensity of these signals remains constant as function of the applied potential. This behavior is quite different than that observed for all other bands in the SFG spectra shown in Fig. 3. In order to investigate whether these peaks are originated at the CaF_2/solution interface, Fig. 4 displays the SFG spectra for the following interfaces: CaF_2/

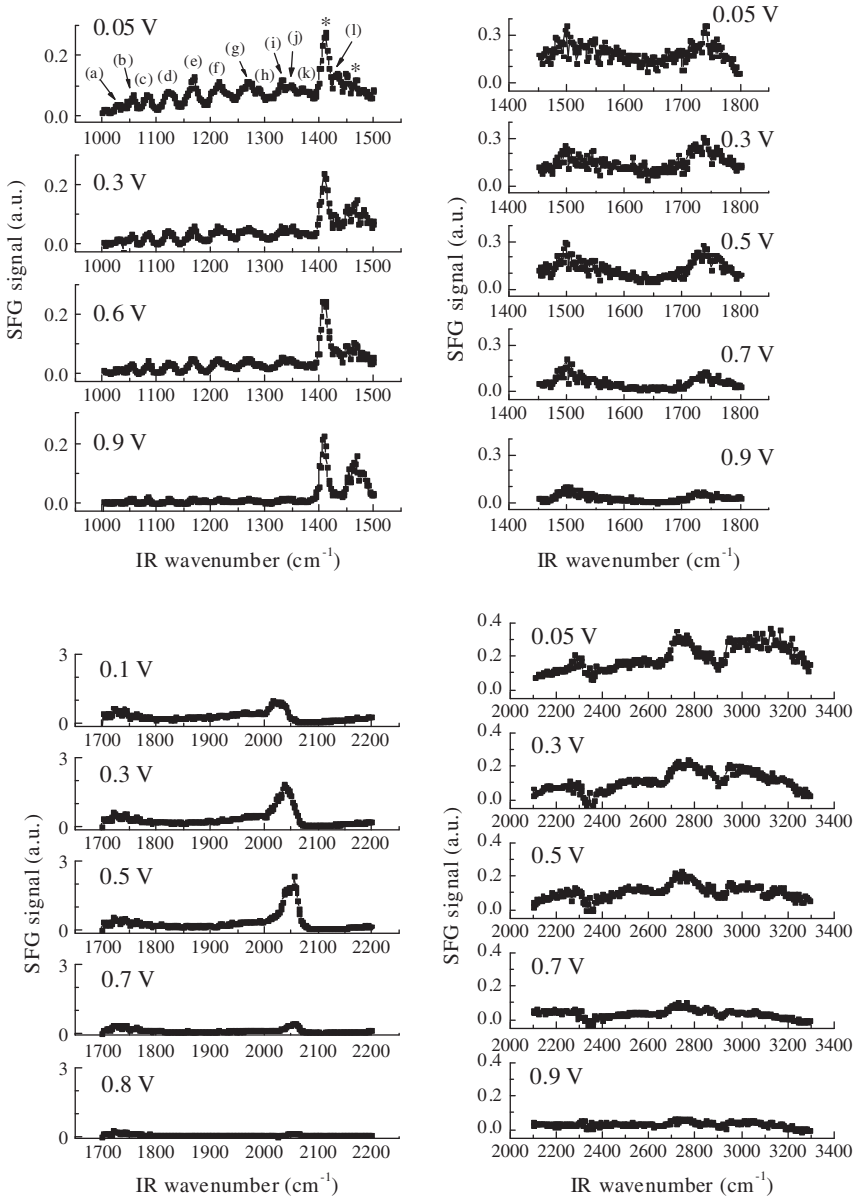

Fig. 5. SFG spectra (1000–3300 cm^{-1}) of the (0.1 mol L^{-1} ethanol + 0.5 mol L^{-1} $HClO_4$)/Pt interface as a function of the applied potential. The potential is indicated in the SFG spectra. Peaks labeled with letters are listed in the text. *The SFG peak at 1408 cm^{-1} and the SFG band at ~1475 cm^{-1} are not related to any molecular vibrational transition (see Section 3.1).

(0.1 mol L^{-1} ethanol + 0.5 mol L^{-1} $HClO_4$)/Pt at 0.05 V vs. RHE (A), CaF_2/0.5 mol L^{-1} $HClO_4$/Pt at 0.05 V vs. RHE (B), CaF_2/air/Pt (C), air/Pt (D), and air/CaF_2 (E). It is important to emphasize that the acquisition of the SFG spectra for the CaF_2/air/Pt, air/Pt, and air/CaF_2 interfaces was performed in this sequence, on the same components, and immediately after a rigorous cleaning of the CaF_2 window (with $KMnO_4$/KOH and H_2O_2/H_2SO_4 solutions, followed by copious rinsing with Milli – Q water) and H_2-flame-annealing the Pt electrode. For the air/CaF_2 interface, the visible pulse energy was increased from 40 to 900 μJ to increase the experimental sensitivity. It can be noted in Fig. 4 that the peak at ~1408 cm^{-1} and the broad band between 1445 cm^{-1} and 1490 cm^{-1} are present in the SFG spectra of the CaF_2/ethanol + $HClO_4$/Pt, CaF_2/$HClO_4$/Pt, and CaF_2/air/Pt interfaces. Nothing is evidenced in the spectra of the air/Pt and air/CaF_2 interfaces.

The presence of these bands in the spectrum for the CaF_2/air/Pt (in the absence of the electrolytic solution!) and their absence for the air/Pt and air/CaF_2 interfaces clearly show that these signals are not due to any organic contamination and are also not originated from molecular resonances of adsorbates from the solution. Instead, they only appear when the CaF_2 window is in close contact with the Pt electrode. A plausible explanation would be that these bands are due to adsorbed species on the CaF_2 window, most likely the OH bending mode of surface CaOH groups, since hydroxyapatite – $Ca_5(PO_4)_3(OH)$ – presents a vibration just above 1400 cm^{-1} [52]. These vibrations would only become apparent when in contact with a rough Pt surface due to local enhancement of the optical field on the metal surface asperities, which would significantly increase the SFG sensitivity. However, this explanation is also unlikely, since the wavenumber of this band did not redshift in presence of deuterated reagents (as shown in Fig. 7, Section 3.3). The origin of these signals at 1408 cm^{-1} and ~1475 cm^{-1} is a very interesting question and clearly more experimental and theoretical work is needed to clarify this issue. Here, we will not investigate this further, since this is not directly relevant to the present study. A more detailed discussion of possible origins of these features can

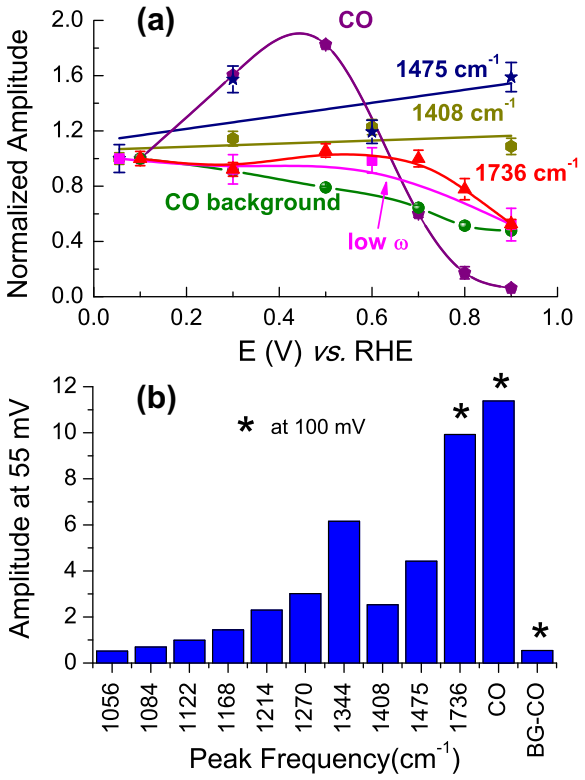

Fig. 6. (a) Normalized amplitudes of the nonresonant background and SFG resonances between 1000 cm^{-1} and 1500 cm^{-1}, and from 1700 to 2200 cm^{-1} (from the theoretical fits of the SFG spectra presented in Fig. 5) as a function of the applied potential. (b) Amplitudes of the various SFG resonances at low potentials.

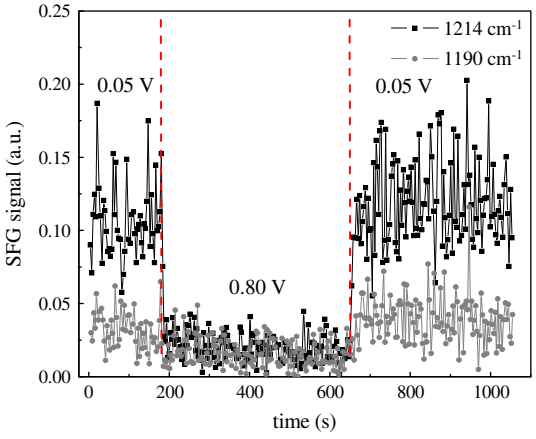

Fig. 7. Intensity of the SFG signals at 1190 cm^{-1} (gray line + gray circles) and 1214 cm^{-1} (black line + black squares) as function of time. The red-dashed lines indicate the exact time of the potential step from 0.05 V to 0.80 V, and back to 0.05 V. (For interpretation of the references to color in this figure legend, the reader is referred to the web version of this article.)

be found elsewhere [51]. Hereafter, we will no longer mention these bands in the discussion, since they are not related to adsorbates on the Pt surface.

3.2. Effect of the applied potential on the SFG spectra

Fig. 5 shows a set of SFG spectra for the (0.1 mol L^{-1} ethanol +0.5 mol L^{-1} $HClO_4$)/Pt interface as a function of the applied potential. The SFG spectra were taken during the first series of increasing potential steps from 0.05 V up to 0.90 V (0.05 V steps) in the wavenumber range between 1000 cm^{-1} and 3300 cm^{-1}.

The SFG spectrum taken at 0.05 V presents more clearly some bands in the wavenumber range between 1000 cm^{-1} and 1500 cm^{-1} that are less evident in the spectra taken at relatively more positive potentials. Particularly in the wavenumber region between 1000 cm^{-1} and 1440 cm^{-1}, SFG bands are observed at: (a) 1030 cm^{-1}, (b) 1056 cm^{-1}, (c) 1084 cm^{-1}, (d) 1122 cm^{-1}, (e) 1168 cm^{-1}, (f) 1214 cm^{-1}, (g) 1270 cm^{-1}, (h) 1288 cm^{-1}, (i) 1330 cm^{-1}, (j) 1348 cm^{-1}, (k) 1370 cm^{-1}, and (l) 1432 cm^{-1}.

In general, it can be noted in Fig. 5 that the intensity of the majority of the bands evidenced between 1000 cm^{-1} and 1800 cm^{-1} and between 2100 cm^{-1} and 3300 cm^{-1} decreases with increasing potential from 0.05 V to 0.90 V vs. RHE. Differently, the intensity of the band assigned to the C≡O stretching mode of the linear-bonded CO molecules (~2050 cm^{-1}) gradually increases until 0.50 V and then starts to decrease. Most of the SFG signals in the wavenumber range from 1000 cm^{-1} to 3300 cm^{-1} are significantly reduced at 0.90 V. As previously mentioned in Section 3.1, the intensity of the peak at 1408 cm^{-1} and the broad band at ~1475 cm^{-1} (not from adsorbates) remains nearly constant with the increasing potential. The broad bands at ~1500 cm^{-1} and ~1740 cm^{-1} are also reduced with increasing potential, but are still noticeable at 0.9 V.

It is noteworthy to mention that the frequency of the C≡O stretching vibration of the linear-bonded CO molecules noticeably blueshifted as function of the increasing potential from 0.1 V to 0.9 V as a result of the vibrational Stark effect [53,54], back-donation mechanism [55], and dipole–dipole coupling effect [28,56]. Due to the high complexity of the SFG spectra ranging from 1000 cm^{-1} to 1800 cm^{-1} and from 2100 cm^{-1} to 3300 cm^{-1}, it is unclear whether the bands other than that at ~2050 cm^{-1} are shifting with the electric field, although any shift may be at most a few wavenumbers.

In order to quantitatively evaluate the effect of the applied potential on the SFG resonances and the nonresonant background from the Pt electrode, the SFG spectra between 1000 cm^{-1} and 1500 cm^{-1} and between 1700 cm^{-1} and 2200 cm^{-1} of the (0.1 mol L^{-1} ethanol + 0.5 mol L^{-1} $HClO_4$)/Pt interface (data presented in Fig. 5) were fitted to the standard Lorentzian model:

$$I_{SFG} \propto \left| Be^{i\phi} + \sum_q \frac{A_q}{\omega_{IR} - \omega_q + i\Gamma_q} \right|^2 \quad (1)$$

where A_q, ω_q, and Γ_q are the strength, resonance frequency and line width of the qth vibrational mode, while ϕ and B are the phase and amplitude of the nonresonant contribution, respectively. In order to reduce the number of adjustable parameters and reduce their uncertainty, all SFG spectra in a given frequency range were fitted simultaneously with the same ϕ, ω_q, and Γ_q (only B and A_q were allowed to vary with potential, except for the CO peak at ~2050 cm^{-1}, which also has a potential-dependent frequency). The SFG spectra between 1700 cm^{-1} and 2200 cm^{-1} were fitted with two resonant signals at ~1750 and ~2050 cm^{-1}. For the frequency range between 1000 cm^{-1} and 1500 cm^{-1}, the data were first corrected for the absorption of the CaF_2 window (see Section 2.1), since this would make it difficult to fit with a *constant* nonresonant background plus resonances. It was then fitted with ten different peaks at 1033 cm^{-1}, 1056 cm^{-1}, 1086 cm^{-1}, 1127 cm^{-1}, 1169 cm^{-1}, 1218 cm^{-1}, 1271 cm^{-1}, 1344 cm^{-1}, 1409 cm^{-1}, and 1457 cm^{-1}. Some of these peaks have contributions from more than one resonance, but they were considered to be a single peak to simplify the theoretical fits, therefore reducing parameter uncertainty. However, peak strengths in SFG spectroscopy are proportional to (A_q/Γ_q). As a result of this, the relative amplitudes A_q from the theoretical fits of the SFG resonances between 1000 cm^{-1} and 1500 cm^{-1} are not accurate,

because they also depend on the bandwidth Γ_q. The amplitude vs. potential behavior is however truthful within the error bars. To fit the two broad bands in the frequency range between 1450 cm^{-1} and 1800 cm^{-1}, it was necessary to include four broad and overlapping peaks, leading to a very large parameter uncertainty. Therefore, they are unreliable and will not be presented or discussed further. Fig. 6a presents the amplitudes of the SFG resonances between 1000 cm^{-1} and 1500 cm^{-1}, at ~1750 cm^{-1} and the CO peak at ~2050 cm^{-1} as a function of the applied potential, normalized to their values at low potentials. Since the peaks from 1000 cm^{-1} to 1400 cm^{-1} have the same potential dependence within the fitting uncertainty, they are represented with an average curve labeled as "low ω". It also displays the potential dependence of the nonresonant background obtained from the spectra between 1700 cm^{-1} and 2200 cm^{-1}, since it is determined more accurately in that frequency range. Fig. 6b presents the A_q for the various resonances at low potentials, to show their relative magnitudes.

The quantitative behavior of the resonant amplitudes as function of the applied potential (as seen in Fig. 6a) shows that the intensity of the CO band increases up to about 0.50 V and then decreases, while the low frequency peaks initially stay constant, but then decrease with increasing potential above 0.70 V vs. RHE. In addition to that, it can be observed in Fig. 6 that the intensity of the nonresonant background also decreases with increasing potential. However, the decrease in the nonresonant contribution is more gradual than that of the low frequency resonant signals, indicating that their potential dependence is not determined by the nonresonant contribution, giving further support to the conclusion that these multiple low frequency peaks are not due to interference effects [51].

Surprisingly, the major part of the adsorbed intermediates of the ethanol electro-oxidation reaction over platinum in acidic medium is formed at 0.05 V. These results show that the platinum surface is highly reactive, even at potential as low as 0.05 V. In the potential range between 0.05 V and 0.40–0.50 V, the small variation of the faradaic current (Fig. 2) shows that adsorbed species are not forming the final products of the reaction. However, in this potential region, there is a gradual increase in the amplitude for the band related to the C≡O stretching vibration of the linearly-bonded CO molecules. This suggests that the CO layer may be formed from the progressive consumption of part of the adsorbed species formed at 0.05 V, although the reduction of amplitudes for the low frequency SFG peaks (Fig. 6) is not obvious (given the large uncertainties), perhaps because there are so many adsorbed species that only a small fraction of each needs to be converted to CO. Therefore, it seems that the adsorbed species formed at 0.05 V are partially transformed into CO with the increasing potential.

At around 0.40–0.50 V, we observe the onset of the faradaic current (Fig. 2). Thus, from this potential, the adsorbed species are removed from the surface, originating the reaction products. In agreement with our results, Wang et al. [57] demonstrated on the basis of Differential Electrochemical Mass Spectrometry (DEMS) data that the formation of acetaldehyde (m/z = 29) begins at 0.40 V vs. RHE, just at the onset potential of the faradaic current. Moreover, they observed that acetaldehyde is produced in a wide range of potentials, including the reserve cycle, whereas the carbon dioxide (m/z = 22) is produced only in the region of potentials between 0.50 V and 0.90 V vs. RHE [57]. This is exactly the potential range where we observe a decrease in the CO peak at 2056 cm^{-1}, supporting the picture that CO_2 is produced mostly from further oxidation of adsorbed CO.

In the oxidation region (between 0.5 V and 0.90 V), we do not observe a dynamic equilibrium between the adsorbed species and the species in the solution. We could expect that the free platinum sites would be replaced by other ethanol molecules as the oxidation of the adsorbed species begins (above 0.50 V). In this way, the reaction would occur dynamically and the intensity of the bands would remain constant as function of the increasing potential. In contrast to this expected behavior, we observe a progressive decrease in the band intensities. This result could be interpreted in three different ways:

(i) The gradual decrease in the SFG band intensities in the oxidation region could be explained by the consumption (at relatively high potentials) of ethanol in the thin layer of electrolytic solution between the platinum electrode and the CaF_2 window, which would then not be available to replenish the adsorbed species after reaction. In this picture, we consider that the rate of ethanol transport from the bulk to the thin layer of electrolytic solution is negligible in comparison with the rate of oxidation of the adsorbed species, leading to the ethanol exhaustion in the thin layer.

(ii) Another possibility is that the electrochemical surface reaction rate is much faster than the diffusion rate of ethanol from the thin layer of electrolyte to the electrode surface. In this case, the steady state concentration of adsorbates would be very low, being below the sensitivity limit of our SFG spectra.

(iii) Alternatively, as the oxidation of the adsorbed intermediates begins, these species are removed from the surface and the free platinum sites are partially reoccupied by different species that are not SFG active in the spectral range we have explored. In this case, these species would poison the platinum surface and act as an ethanol oxidation inhibitor.

Considering the scenario (i) above, we now estimate the time required to consume most of ethanol molecules in the thin layer volume by electrochemical oxidation at 0.80 V. The initial current density in a chronoamperometry curve for potentials in the ethanol oxidation peak (0.8 V) is of the order of 1 mA/cm^2. [34] Therefore, the faradaic charge that passes through the working electrode (area ~1 cm^2) during one second is ~1 mC, which corresponds to 1.04×10^{-8} mol of electrons. According to Wang et al. [57], the product yield of the 0.1 mol L^{-1} ethanol oxidation reaction on platinum in acidic medium (over a full potential cycle) is equivalent to: 1.3%, 55% and 44% for carbon dioxide, acetaldehyde and acetic acid, respectively. Considering these product yields and the number of electrons produced in each reaction (12 e^-, 2 e^- and 4 e^- for ethanol → CO_2, ethanol → acetaldehyde and ethanol → acetic acid, respectively), the average number of electrons produced per oxidized ethanol molecule is 3. With that, 1.04×10^{-8} mol of electrons will be produced in the electro-oxidation of 3.47×10^{-9} mol of ethanol molecules. For estimating the electrolytic solution volume, we take the thin layer thickness as 1 μm, which yields a volume of 1×10^{-4} cm^3. At 0.1 mol L^{-1}, the amount of ethanol present in the thin layer is 1×10^{-8} mol. Therefore, this crude estimate indicates that it would take about 3 s to consume all the ethanol in the thin layer of solution between the electrode and the CaF_2 window. We will describe below an experiment designed to investigate the time evolution of the SFG spectra upon a potential step, which may address this issue.

Fig. 7 shows the intensity of the SFG signals at 1190 cm^{-1} and 1214 cm^{-1} as function of time. The curves were acquired simultaneously, with the OPA tuned back and forth between the two frequencies, and the time interval between two subsequent points in each curve is about 3 s. In this experiment, the electrode potential was changed from 0.05 V to 0.80 V and then, after almost 500 s, from 0.80 V back to 0.05 V. The SFG signals at 1190 cm^{-1} and 1214 cm^{-1} correspond to a valley between two nearby resonances and to one of the intense resonances shown in Fig. 5, respectively. On one hand, the SFG signal at 1190 cm^{-1} serves as a guide for the

nonresonant signal of the platinum electrode at 0.05 V and 0.80 V. On the other hand, the signal at 1214 cm^{-1}, related to adsorbed intermediates of the ethanol oxidation over platinum, monitors the lifetime of the adsorbed species when the potential is changed from 0.05 V to 0.80 V and also the time required to re-establish the layer of adsorbed molecules when the potential is changed from 0.80 V to 0.05 V.

It can be noted in Fig. 7 that the intensity of the SFG signals at 1190 cm^{-1} and 1214 cm^{-1} remains constant as function of time at 0.05 V and quickly decreases when the potential is changed from 0.05 V to 0.80 V. The abrupt change in the SFG signal is consistent with an instantaneous jump, within the temporal resolution of the measurement (~3 s). The ratio between the intensities of the SFG signal at 0.05 V and 0.80 V is equal to 2 and 6.5 for the nonresonant signal of the platinum (1190 cm^{-1}) and the SFG signal at 1214 cm^{-1}, respectively. When the potential is changed from 0.80 V to 0.05 V, the original situation is instantaneously retrieved (again, within the temporal resolution of the measurement, ~3 s). This experiment was repeated in triplicate and the obtained results were in accord with those presented in Fig. 7. Also, the same behavior was observed for the SFG signal at 1120 cm^{-1}.

Although the fast decrease in the SFG signal at 1214 cm^{-1} is consistent with the hypothesis of ethanol consumption and our estimate of its timescale, the similarly fast recovery of this signal would not be expected, since it would take place in the much slower timescale of the diffusion of ethanol from the bulk solution into the thin layer of electrolyte. On the other hand, if our estimate of the timescale for ethanol consumption in the thin layer is too short, we should then have observed a gradual decrease in the SFG signal upon increasing the potential from 0.05 V to 0.8 V. Thus, we can rule out the exhaustion of the ethanol molecules in the thin layer of electrolyte as the reason for the decrease in the intensity of the most of the SFG bands at the wavenumber range between 1000 cm^{-1} to 3300 cm^{-1} from 0.50 V to 0.90 V (Fig. 5).

We believe the most appropriate explanation is given by scenario (iii) above, that is, the adsorbed intermediates from ethanol oxidation are gradually oxidized with increasing potential, and the free platinum sites are not re-occupied only by ethanol molecules, but also by other species that poison the catalyst surface, suppressing the dynamic oxidation reaction via adsorbed intermediates. This is in fact what is observed in chronoamperometry experiments, where a marked reduction in the oxidation current is observed at a fixed potential within the ethanol oxidation peak [34]. However, these poisoning species are not detected by SFG spectroscopy, probably because their vibrations are below 1000 cm^{-1} (e.g., Pt—O). As the potential increases, the relative coverage of ethanol adsorbates to the poison species decreases, and at 0.90 V, most of the adsorbed intermediates were completely removed from the platinum surface (very weak SFG signals in Fig. 5), and the faradaic current starts to decrease in the cyclic voltammogram shown in Fig. 2. The immediate recovery of the SFG signal when the potential is changed from 0.8 V back to 0.05 V shows that the poison is readily reduced and leaves the Pt surface ready for ethanol readsorption. Additionally, the reduction of the SFG peak intensities could also be due to a low dynamic coverage of the intermediates during the oxidation reaction, as a result of a faster oxidation turnover with respect to local ethanol diffusion and adsorption (scenario (ii)). However, this cannot be the only mechanism to explain the reduction in SFG signal at 0.8 V, since this would imply on a constant oxidation current, which is inconsistent with chronoamperometry experiments.

At this point, another interesting question appears: if we do not observe most of the SFG bands related to the adsorbed intermediates of the ethanol electro-oxidation reaction on platinum above 0.90 V, how could we explain the second oxidation peak (at around 1.30 V) in the cyclic voltammogram shown in Fig. 2, which corresponds to a reactivation of the electrode for ethanol oxidation? Above 0.90 V, it is possible that the adsorbed reaction intermediates are different than those observed at relatively lower potentials. The conversion of part of the adsorbed intermediates (formed at 0.05 V) to other adsorbed species, in particular linear-bonded CO, is a proof that the reaction mechanism depends on the applied potential. Additional evidences were reported by Wang et al. [57] and Iwasita [58]. They investigated the volatile products (acetaldehyde and carbon dioxide) of the ethanol electro-oxidation over platinum using DEMS and they observed that only acetaldehyde is formed above 1.10 V. In this potential region, probably the adsorption of ethanol molecules and the C—C bond breaking are inhibited by the presence of other species adsorbed on the platinum surface. As a result, the intermediates are weakly adsorbed (little residence time at the surface) and quickly transformed into partially oxidized products. In such a manner, we do not observe the SFG bands associated with the reaction intermediates in the potential range between 1.10 V and 1.30 V due to their low steady-state surface coverage, below the sensitivity of our SFG apparatus. Therefore, we are not able to explore these adsorbed species and offer a mechanistic view of the Pt reactivation at 1.10 V. It is important to mention that Ohmic drop effects could affect the region of faradaic current, above 0.5 V vs. RHE, increasing the applied potential necessary to attain the desired electrode potential E. Therefore, when we use 0.9 V in the thin film geometry, it may actually correspond to a *lower* electrode potential vs. RHE. We did not correct our results for the ohmic drop. However, neglecting this correction does not affect our qualitative analysis on the formation/reactivity of adsorbed intermediates of the ethanol electro-oxidation on Pt.

Finally, we discuss the thermodynamic implications of our findings. At first, it seems quite surprising that several adsorbates coexist simultaneously at low potentials, as implied by the complex SFG spectra in the 1000–1400 cm^{-1} range. This would require that many adsorbates would have similar adsorption free energies, so that their equilibrium surface coverages are comparable. However, this unlikely conclusion assumes thermodynamic equilibrium between the adsorbates and ethanol in solution. If the adsorption energies are high enough when compared to the thermal energy, the adsorption would be "irreversible" (at a fixed potential), and the surface coverages would not be determined by thermodynamic equilibrium, but rather by the kinetics of adsorption and reaction. In this way, all adsorbates that have high adsorption energies would have appreciable coverage, despite any difference in their energy values.

3.3. Results with isotopically labeled ethanol

In order to assist the peak assignment of the SFG spectra, especially in the fingerprint region, we have performed experiments with deuterium labeled reagents (water and ethanol) and also ^{13}C labeled ethanol. Fig. 8 shows the SFG spectra from 1000 cm^{-1} to 1800 cm^{-1} and from 2100 cm^{-1} to 3300 cm^{-1} of the following interfaces: (0.1 mol L^{-1} CH_3CH_2OH + 0.5 mol L^{-1} $HClO_4$)/Pt and (0.1 mol L^{-1} CD_3CD_2OD/D_2O + 0.5 mol L^{-1} $HClO_4/D_2O$)/Pt. All SFG spectra presented in Fig. 8 were taken at 0.3 V vs. RHE. SFG spectra ranging from 1000 cm^{-1} to 1500 cm^{-1} of the (0.1 mol L^{-1} CH_3CH_2-OH + 0.5 mol L^{-1} $HClO_4$)/Pt interface and (0.1 mol L^{-1} CH_3—$^{13}CH_2$-OH + 0.5 mol L^{-1} $HClO_4$)/Pt interface at 0.05 V vs. RHE are presented in Fig. 9. Table 1 summarizes the wavenumbers of the main bands evidenced in the SFG spectra presented in Figs. 8 and 9. It also includes possible band assignments that will be discussed in Section 3.4.

As seen in Fig. 8, the SFG spectrum for CD_3CD_2OD + $HClO_4$/Pt presents most of the bands observed in the wavenumber region between 1000 cm^{-1} and 1450 cm^{-1} for the CH_3CH_2OH + $HClO_4$/Pt

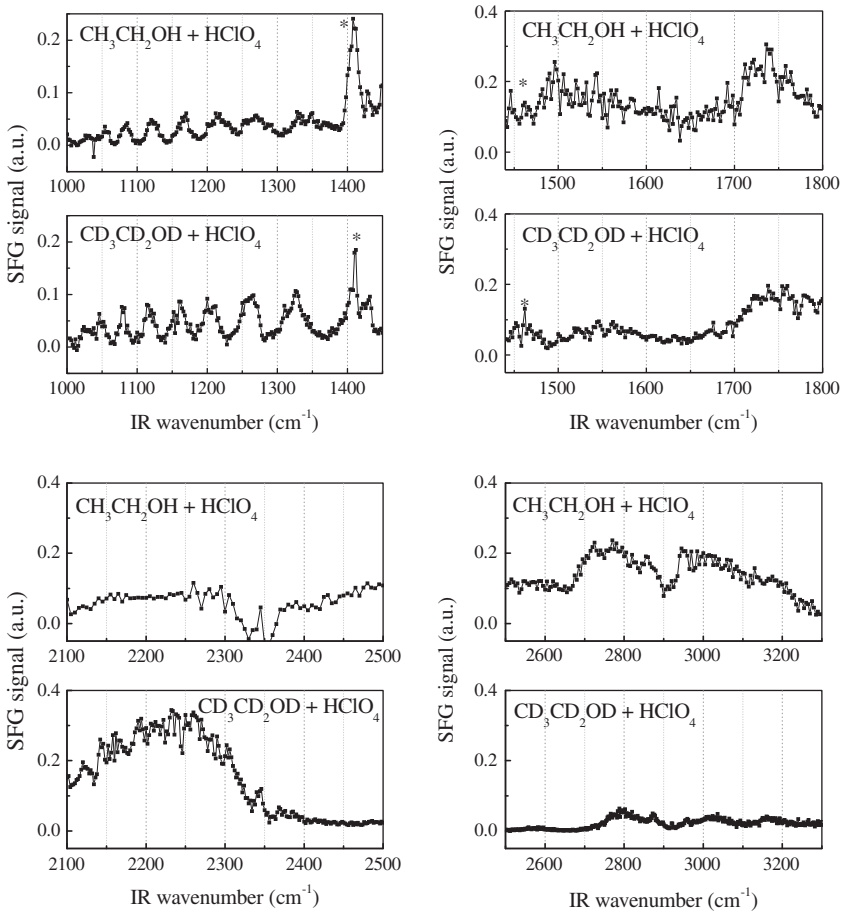

Fig. 8. SFG spectra (1000–1800 cm^{-1} and 2100–3300 cm^{-1}) of the following interfaces: (0.1 mol L^{-1} CH_3CH_2OH + 0.5 mol L^{-1} $HClO_4$)/Pt and (0.1 mol L^{-1} CD_3CD_2OD in D_2O + 0.5 mol L^{-1} $HClO_4$ in D_2O)/Pt at 0.30 V vs. RHE. *The SFG peak at 1408 cm^{-1} and the SFG band at ~1475 cm^{-1} are not related to any molecular vibrational transition (see Section 3.1).

spectrum, except the SFG bands at 1288 cm^{-1}, 1348 cm^{-1} and 1370 cm^{-1}. From 1450 cm^{-1} to 1800 cm^{-1}, the main change in the $CD_3CD_2OD + HClO_4$/Pt spectrum compared to the CH_3CH_2-$OH + HClO_4$/Pt interface spectrum is the absence of the band at around 1496 cm^{-1}. In the wavenumber range between 2100 cm^{-1} and 2500 cm^{-1} for the deuterated solution (only the $HClO_4$ was protonated), it can be noted a broad band (from 2100 cm^{-1} to 2350 cm^{-1} centered at ~2250 cm^{-1}), which may be due to the OD stretch of water molecules interacting with the Pt surface by hydrogen bonding, that is, the same band at 2700–3300 cm^{-1} for $CH_3CH_2OH + HClO_4$/Pt but red shifted upon deuteration. Finally, between 2500 cm^{-1} and 3300 cm^{-1}, the CD_3CD_2 $OD + HClO_4$/Pt spectrum presents relatively less intense bands than the $CH_3CH_2OH + HClO_4$/Pt spectrum, since the H abundance in the solution is much smaller. In presence of CH_3—$^{13}CH_2OH$ (as shown in Fig. 9), bands in the wavenumber range between 1000 cm^{-1} and 1500 cm^{-1} are red shifted with respect to the band positions for $CH_3CH_2OH + HClO_4$/Pt.

The results with isotopically labeled ethanol are extremely important for the identification of the adsorbed intermediates of the ethanol electro-oxidation on Pt in acidic medium. On one hand, the bands present in both CH_3CH_2OH/Pt and CD_3CD_2OD/Pt spectra definitively correspond to C—C and C—O vibrational modes of the adsorbed intermediates. On the other hand, the bands that disappear in the presence of deuterated ethanol and D_2O are surely related to C—H and O—H vibrational modes. The ^{13}C results indicate that most of the adsorbed intermediates detected between 1000 cm^{-1} and 1500 cm^{-1} present the carbon atom initially attached to the OH group of the ethanol (α carbon), although the partial overlap between the displaced bands (^{13}C) and the original bands (^{12}C) may allow a contribution from species containing only ^{12}C (the β carbon of ethanol).

3.4. Tentative Assignment of the Vibrational Bands and Identification of Reaction Intermediates

Based on the results with isotopically labeled ethanol, which were presented in the last section, we have discussed only the general assignment of the vibrational SFG bands observed in the present work. The detailed discussion of them is relatively more complex. For this reason, we need support from literature and theoretical calculations.

In order to have supporting information for the assignment of the observed peaks in the SFG spectra for the ethanol solution/Pt interface (listed in Table 1), we theoretically evaluated the infrared and Raman spectra of some of the possible adsorbed intermediates of the ethanol electro-oxidation on Pt. The species considered here were: carbon monoxide, a secondary ethanol derivative (Pt—CHOH—CH_3), a tertiary ethanol derivative [$(Pt)_2$=COH—CH_3], acetyl, bidentate acetate, ethoxy and η^2-acetaldehyde. Although the accurate computation of IR and Raman intensities is notoriously difficult, the theoretical results for fundamental frequencies usually show satisfactory agreement (within a few tens of cm^{-1}) with the experimental data [44,59]. As a benchmark calculation, we have computed the infrared and Raman spectra for an isolated ethanol molecule to compare them with experimental results for

Table 1
Wavenumber of the main bands observed in the SFG spectra shown in Fig. 8 and Fig. 9.

CH_3CH_2OH (CD_3CD_2OD) on Pt/ cm^{-1} (this work)	CH_3 $^{13}CH_2OH$ on Pt/cm^{-1} (this work)	Adsorbates (deuterated adsorbates) on metal surfaces [Ref.]/cm^{-1}	Assignment [Ref.]*,a,b	Proposed adsorbed intermediate
1030 (1024)	1022	1030 [73,74,91]	ν(C—O) [82–84,91] ν(C—C) + ν(C—O) [73,74]	Methoxy [82–84,91], ethoxy [73,74]
1056 (1050)	1048	1055 (1070) [69] 1045*	ν(C—C) $\rho(CH_3)$ + ν(C—C) + ν(C—O)*	Bidentate acetate [69], secondary ethanol derivative*
1084 (1082)	1078	1068*	ν(C—C) + δ(OH)*	Tertiary ethanol derivative*
1122 (1116)	1114	1135 (1115) [72], 1127* 1120–1160 [79]	ν(C—C) [72] ν(C—C) + $\rho(CH_3)$* ν(C—C) [79]	η^2-Acetaldehyde [72], acetyl*, ethylidyne [79]
1168 (1162)	1160	1155* 1163 [80]	δ(OH) + ν_s(O—C—C) + $\rho(CH_3)$* ν(C—C) [80]	Tertiary ethanol derivative* ethylidyne [80]
1214 (1210)	1204	1200 [85]	ν(C—OH) [85]	Tertiary methanol derivative [85]
1270 (1270)	1250	1270 [85,86]	ν(C—OH)	COH residues [85,86]
1288 (not seen) 1330 (1326)	1266 1310	1262, 1280* 1320 [87–90], 1360*	δ_{ip}(CH) + $\rho(CH_3)$* $\nu_s(COO^-)$ [87–90] ν(C—C) + $\nu_s(COO^-)$*	Secondary ethanol derivative,* η^2-acetaldehyde* Bidentate formate [87–90], bidentate acetate*
1348 (not seen)	1326	1350 [92], 1353*	ω (CH_2) [92] $\delta_s(CH_3)$*	Ethoxy [92], acetyl*
1370 (not seen)	1346	1370 [72–74,78],*	$\delta(CH_3)$	methoxy [78], ethoxy [73,74], η^2-acetaldehyde [72], bidentate acetate,* secondary and tertiary ethanol derivative*
1432 (1430)	1430	1415–1420 [78]	ν_{ip}(C—O) [78]	η^2-Formaldehyde [78], η^2-acetaldehyde [78] η^2-acetyl
1496 (not seen)		1499 [71]	$\delta_s(CH_2)$ [71]	Ethoxy [71], CH_2(ads)
1546 (1546)		1565 (1595) [77]	ν(C═O)	Acetyl [77]
1736 (1736)		1735 [81], 1745[87]	ν(C═O)	Monodentate acetate [81], monodentate formate [87]
2056 (2100–2350)		2055–2070 [13,16,19]	ν(C≡O) ν(OD)	Adsorbed CO [13,16,19] Adsorbed D_2O
2700–3300 (weak)		2700 [49,50] (broad) 2670 [48], 2900 [47] (broad)	ν(OH)	Adsorbed H_2O, H_3O^+

* Wavenumbers and assignments from theoretical calculations carried out in the present work.
[a] Notation used for mode description: ν, stretching; δ, deformation; ω, wagging; ρ, rocking.
[b] Subscripts indicate the type of mode: s – symmetric, as – asymmetric, op – out-of-plane vibration, ip – in-plane vibration.

(liquid) ethanol [60–62] and check the accuracy of our method. The theoretical results are shown in Tables 2 and 3.

Table 2 presents experimental and calculated wavenumbers corresponding to ethanol vibrations. In addition, the differences between experimental and calculated wavenumbers (considering the scale factor or not) are also presented in Table 2. In both cases, it can be noted that the differences between experimental and calculated wavenumbers are not uniform for low and high wavenumber regions. By analyzing these differences without the scale factor, it can be seen that the calculation obtains frequency values closer to those observed experimentally in the region corresponding to the C—C and C—O vibrations. Therefore, in the following discussion of SFG peak assignments (Table 1) we have not used the scale factor in comparisons between experimental and calculated wavenumbers for vibrations involving C—C and C—O stretches. On the other hand, in the wavenumber regions corresponding to CH vibrations, the unscaled calculation overestimates the experimental frequencies and the scaled calculated wavenumbers show good agreement with experiment. In this way, for CH vibrations, we have used the scaled calculated frequencies when comparing to experimental peaks listed in Table 1. It is important to mention that for OH vibrations, the calculation estimates wavenumber values very far from those observed experimentally (considering the scale factor or not). This is obviously due to the fact that hydrogen bonding of the OH group to other ethanol or water molecules is not taken into account in our calculations. Therefore, theoretical frequencies which involve OH vibrations will not be used for comparisons with experiments.

As shown in Table 3, there is satisfactory agreement between the theoretical results for CO on Pt (2002 cm^{-1}) with the experimental data (2056 cm^{-1}), especially considering that this vibration is coverage- and potential-dependent, effects which have not been

Table 2
Experimental results and theoretical predictions for ethanol. Only the resonances that are intense in both IR and Raman spectra are listed.

Experimental [60–62] (cm^{-1})	Theoretical wavenumbers unscaled (scaled)[a] (cm^{-1})	Assignment[b,c]	$\Delta_{exp.\ -\ unscaled}$	$\Delta_{-\ exp.\ -\ scaled}$
882	896 (860)	ν_s(CCO)	−14	+22
1051	1034 (993)	ν_a(CCO)	+17	+58
1094	1094 (1050)	ν_s(CO)	0	+44
1320	1270 (1219)	δ(COH)	+50	+101
1383	1449 (1391)	$\omega(CH_2)$, $\delta_s(CH_3)$	−66	−8
1454	1502 (1442)	$\delta_{as}(CH_3)$	−48	+12
2877	2963 (2844)	$\nu_s(CH_2)$	−86	+33
2890	2989 (2869)	$\nu_a(CH_2)$	−99	+21
2928	3017 (2896)	$\nu_s(CH_3)$	−89	+32
2974	3082 (2959)	$\nu_a(CH_3)$	−108	+15
2974	3089 (2965)	$\nu_a(CH_3)$	−115	+9
~3350	3794 (3642)	ν_s(OH)	−444	−292

[a] Scale factor 0.96 [93].
[b] Notation used for mode description: ν, stretching; δ, deformation.
[c] Subscripts indicate the type of mode: s – symmetric and as – asymmetric.

Table 3
Theoretical predictions for CO, secondary and tertiary ethanol derivative, acetyl, bidentate acetate, ethoxy and η^2-acetaldehyde adsorbed on Pt(111). Only the resonances that are intense in both IR and Raman spectra are listed. Underlined values will be considered in comparison with experimental peaks (see text for details).

Adsorbates	Theoretical wavenumbers unscaled (scaled)[a] (cm^{-1})	Assignment[b,c]
CO	2002 (1922)	ν(C≡O)
Secondary ethanol	1035 (994)	ν(C—C) + δ(CH_3) + δ(OH)
	1045 (1003)	ρ(CH_3) + ν(C—C) + ν(C—O)
	1188 (1140)	Strong δ_{op} (CH) + δ(OH) + weak ρ(CH_3)
	1229 (1180)	Strong δ(OH) + δ_{op} (CH) + weak ρ(CH_3)
	1315 (1262)	Strong δ_{ip}(CH) + weak ρ(CH_3)
	1430 (1373)	δ_s(CH_3)
	1493 (1433)	Strong δ_{as}(CH_3)
	1499 (1439)	δ_{as}(CH_3)
Tertiary ethanol	1017 (976)	ρ_{op} (CH_3) + δ(OH)
	1066 (1023)	ρ_{ip} (CH_3) + δ(OH)
	1068 (1025)	ν(C—C) + δ(OH)
	1203 (1155)	δ(OH) + ν_s(O—C—C) + ρ(CH_3)
	1426 (1369)	δ_s(CH_3)
Acetyl	1037 (996)	ρ(CH_3)
	1127 (1082)	ν(C—C) + ρ(CH_3)
	1409 (1353)	Strong δ_s(CH_3)
	1753 (1683)	ν(C=O) + δ_{as}(CH_3)
Bidentate acetate	1360 (1306)	ν_s(COO^-) + ν(C—C)
	1407 (1351)	Strong ν_{as}(COO^-) + δ(CH_3)
	1428 (1371)	δ_s(CH_3)
Ethoxy	1027 (986)	ν(C—C) + ν(C—O)
	1115 (1070)	ρ(CH_3)
	1271 (1220)	τ(CH_2)
	1370 (1315)	ω(CH_2)
	1419 (1362)	δ_s(CH_3)
	1498 (1438)	δ_{as}(CH_3)
	1508 (1448)	δ_s(CH_2) + weak δ_s(CH_3)
η^2-acetaldehyde	1101 (1057)	ν(C—C)
	1159 (1113)	ρ(CH_3) + ρ_{op}(CH)
	1333 (1280)	strong δ(CH) + weak ρ(CH_3)
	1425 (1368)	δ_s(CH_3)
	3024 (2903)	ν_s(CH_3)

[a] Scale factor 0.96 [93].
[b] Notation used for mode description: ν, stretching; δ, deformation; ω, wagging; τ, twisting; ρ, rocking and *sci*, scissoring.
[c] Subscripts indicate the type of mode: s – symmetric, as – asymmetric, op – out-of-plane vibration, ip – in-plane vibration.

included in the calculations. This validates the methodology employed in the present work. However, the most important conclusion from the theoretical results is that no single adsorbate (nor a small set of them) can explain the very complex vibrational spectra of Fig. 8 in the 1000–1400 cm^{-1} range, particularly knowing that most of these bands are C—C or C—O stretches (as discussed in Section 3.3). We must conclude that it is originated from several adsorbates being present on the Pt surface, even at low potentials. The implications of this finding will be discussed later.

Next, we will discuss in detail the tentative assignments of the SFG bands observed in the present work. These band assignments will be based on our theoretical calculations and on electrochemical and UHV studies previously reported in the literature. We organize the band assignments in following Sections 3.4.1–3.4.4.

3.4.1. Water, hydronium and OD (bands between 2300 cm^{-1} and 3300 cm^{-1})

The broad band from 2650 cm^{-1} to 3200 cm^{-1} may be due to OH stretches of water molecules or hydronium ions (H_3O^+) [47–50] interacting with the Pt surface by hydrogen bonding (not chemisorbed). This band was previously reported in SFG studies [49,50] and assigned to the OH stretching vibration of the water molecules in the double layer. Indeed, the OH stretching vibration frequency of the water molecules in the double layer may be relatively different compared to that observed for liquid water (~3400 cm^{-1}) [63]. However, we disagree with this interpretation for two reasons: (i) the profile of the SFG band related to water in the double layer has been previously reported [23,24] and it is not exactly the one we observe; (ii) the dependence of the band intensity with the potential is not the one expected for water in the double layer. From a negatively charged surface (at low potential) to a positively charged surface (at high potential), we should have observed a decreasing, and then increasing, band intensity, which is also not the case.

3.4.2. Adsorbed intermediates previously proposed at electrochemical environment with basis on electrochemical evidences (ClO_4^-, tertiary ethanol derivative, bidentate acetate, and CO)

The band at 1120 cm^{-1} is extensively reported in the literature [14,20,64,65] and has been assigned to the asymmetric stretching of perchlorate anions in solution. Nevertheless, in the present work, this band presents atypical behavior as a function of the potential (data shown in Fig. 5), compared to previous work [66]. Specifically, the SFG spectra show that the band at 1120 cm^{-1} is present even at potential as low as 0.05 V. Further, its intensity decreases with positive going potential, in contrast to what we can expect for an anion [66]. In fact, another band at 980 cm^{-1} has been observed with SFG spectroscopy and was assigned to absorbed perchlorate anions [33]. Therefore, the feature at 1120 cm^{-1} is more likely to be related to another adsorbed species. The tentative assignment of this feature will be presented later in Sections 3.4.3 and 3.4.4.

According to our calculations, the bands at 1084 cm^{-1} and 1168 cm^{-1} correspond, respectively, to the ν(C—C) + δ(OH) and the δ(OH) + ν_s(O—C—C) + ρ(CH_3) modes of a tertiary ethanol derivative, $(Pt)_2$=COH—CH_3. The latter mode has a strong contribution of the OH bending vibration. For this reason, the scaled theoretical wavenumber in Table 3 is more appropriate than the unscaled one. However, the wavenumber shift in presence of deuterated reactants is only 6 cm^{-1} (Table 1), not as important as we should expect for a mode including a hydrogen atom. With basis on our calculations, we explain this conflicting behavior in terms of the geometry of the adsorbed tertiary ethanol intermediate and the important contribution of the O—C—C stretching to the mode at 1168 cm^{-1}. The OH bond is almost parallel to the platinum surface. Then, although the OH bending is very strong, it contributes not much to the observed peak intensity, according to the infrared selection rule that allows only those vibrations with dipole changes perpendicular to the surface to be observed. Consequently, the character of O—C—C stretching mode, which does not involve any H atom, prevails over the character of OH bending. Therefore, deuteration of the OH group would decouple it from this mixed vibrational mode, without affecting its frequency significantly. Tertiary ethanol derivative was previously proposed by Iwasita and Pastor based on a band at 1257 cm^{-1} assigned to its C—OH stretch [17]. Iwasita and Pastor mentioned that this frequency was slightly higher than that one expected for tertiary ethanol in solution between 1205 cm^{-1} and 1125 cm^{-1}. Therefore, we agree with the possible formation of this intermediate, but disagree on the assignment of the band at 1257 cm^{-1} (see Section 3.4.4).

The band at 1330 cm^{-1} can be attributed to symmetric $\nu(COO^-) + \nu(C—C)$ mode of bidentate acetate, according to our theoretical predictions. Usually, the symmetric $\nu(COO^-)$ vibration mode of adsorbed acetate ions is at relatively higher wavenumbers, near 1420 cm^{-1}, as reported in an FTIR study on the adsorption of acetate at the basal planes of platinum single-crystal electrodes [67]. Recently, the Wieckowski group has also observed acetate vibrations at ~1410 cm^{-1} on Pt and Au electrodes with SFG spectroscopy, with bandwidths from 30 to 50 cm^{-1} [35]. Based on the usual frequency of adsorbed acetate ions, acetate was previously proposed as an adsorbed intermediate of the ethanol electro-oxidation on Pt in acidic medium [13,68]. This species is reported to be formed when acetic acid, one of main soluble products of the ethanol oxidation, becomes adsorbed on Pt. In these studies [13,68], the intensity of the band related to the symmetric $\nu(COO^-)$ mode of bidentate acetate increases as function of the increasing potential, just the opposite tendency we observe in the present study. These differences concerning the wavenumber and potential tendency may be related to the fact that in our study, bidentate acetate species are formed on the surface (by the recombination of the residues from ethanol dissociation on the platinum surface). This situation is particularly different with respect to that one in which acetate adsorbs on platinum as a consequence of the electrostatic attraction between the positively charged surface and acetate anions in solution (from acetic acid ionization). The wavenumber redshift we verify in the present study may be due to the stronger interaction between the platinum surface and oxygen atoms of the acetate formed *in-loco* than that one existing between the platinum surface and adsorbed acetate ions that came from solution, in which the negative charge is expected to be more delocalized between the carbon and oxygen atoms. The unusual potential tendency we observe here is attributable to the consumption of the bidentate acetate, which is a precursor for the formation of other adsorbed intermediates and/or reaction products. Besides the band at 1330 cm^{-1}, the band at 1056 cm^{-1} can be assigned to the C—C stretching mode of bidentate acetate. This assignment is in accord with UHV studies of acetate adsorption on Al(1 1 1) [69] and Cu(1 0 0) [70]. Therefore, based on the evidences of the bands at 1330 cm^{-1} and 1056 cm^{-1}, we suggest that the bidentate acetate is one of the adsorbed intermediates of the ethanol electro-oxidation over platinum in acidic medium.

As mentioned before in Section 3.1, the strong band at 2056 cm^{-1} has been widely reported in the literature [13,16,19] and is attributed to the C≡O stretching mode of CO molecules linearly bonded to the Pt electrode.

3.4.3. Adsorbed intermediates previously proposed at electrochemical environment without any clear experimental evidence (ethoxy, secondary ethanol derivative and acetyl)

The SFG bands at 1030 cm^{-1}, 1348 cm^{-1}, and 1496 cm^{-1} can correspond to the O—C—C stretching mode [ν(C—O) and ν(C—C) coupling], CH_2 wagging and CH_2 deformation of ethoxy species, respectively. This result is in excellent agreement with theoretical calculations for ethoxy adsorbed on Mo(1 1 0) [71] and also in agreement with previous UHV studies of ethoxy adsorbed on Rh(1 1 1) [72], Cu(1 0 0) [73], Mo(1 1 0) [74], and Cu(1 1 1) [75]. Formerly, ethoxy has been suggested as an intermediate of ethanol oxidation on Pt at electrochemical environments, but only on the basis of a band at 2920 cm^{-1}, in the C—H stretching region [17]. Given the well-known difficulty of unambiguously assigning bands in the C—H stretching region [76], the current observation of the SFG bands at 1030 cm^{-1}, 1348 cm^{-1} and 1496 cm^{-1}, which are also supported by our theoretical calculations, provides additional evidence of the presence of ethoxy.

In addition to providing the new and coherent evidences of the presence of ethoxy species adsorbed on platinum in electrochemical environment, the SFG spectra also provide us with evidence of bands at 1056 cm^{-1} and 1288 cm^{-1}, also never before reported in electrochemical studies. These vibrational modes can be related to the secondary ethanol intermediate (Pt—CHOH—CH_3). According to our calculations, the bands at 1056 cm^{-1} and 1288 cm^{-1} could correspond to the [$\rho(CH_3) + \nu$(C—C) + ν(C—O)] and [strong δ_{ip}(CH) + weak $\rho(CH_3)$], respectively. Previously, Iwasita and Pastor [17] have already proposed that ethanol was adsorbed through the α-carbon after the rupture of a C—H bond to form an adsorbed secondary alcohol derivative. However, no evidence for the presence of a secondary ethanol intermediate in the electrochemical environment has been provided in that work [17].

Finally, the formation of acetyl, which was also previously proposed as an intermediates of ethanol oxidation in electrochemical environment (without any clear experimental evidence) [17,68], is consistent with the presence of the bands at 1122 cm^{-1}, 1348 cm^{-1}, and 1546 cm^{-1}. Based on our calculations, the bands at 1122 cm^{-1} and 1348 cm^{-1} can be assigned to [ν(C—C) + $\rho(CH_3)$] and strong $\delta_s(CH_3)$ modes of an acetyl species, respectively. The band at 1546 cm^{-1} was formerly assigned to the C=O stretching mode of acetyl intermediates, which have been detected following the adsorption of acetaldehyde on Pd(1 1 1) in UHV [77]. Our calculation shows that this vibrational mode should occur close to 1750 cm^{-1}. However, given the fact that our calculation does not take into account neither the electrochemical potential nor the active site of platinum, we believe that the band at 1546 cm^{-1} is more likely to be associated with the C=O of an acetyl. Once C=O is directly bonded to the negatively charged platinum surface, the π electrons involved in the double bond, which are more movable than the σ electrons shared in a single bond, can resonate between platinum, carbon, and oxygen atoms. In this case, the interaction between carbon and oxygen atoms has a character of a 1.5 bond and its C—O stretch may occur at around 1550 cm^{-1} (such as the typical asymmetric stretching mode of COO^-).

3.4.4. Adsorbed intermediates of ethanol electro-oxidation proposed in the present work for the first time (η^2-acetaldehyde, η^2-acetyl, ethylidyne, monodentate acetate, methoxy, tertiary methanol derivative, COH residue, η^2-formaldehyde, mono and bidentate formate, CH_3 and CH_2 residues)

The formation of η^2-acetaldehyde (in the η^2-geometry, both the C and O atoms interact with the Pt surface through the carbonyl π orbital) as an adsorbed intermediate of the ethanol oxidation on Pt in acidic medium is compatible with the presence of the bands at 1122 cm^{-1}, 1288 cm^{-1}, and 1432 cm^{-1}. Here, we attribute the bands at 1122 cm^{-1} and 1288 cm^{-1} to the C—C stretching and CH in-plane bending vibrations of the η^2-acetaldehyde, respectively, which are theoretically predicted to be at around 1100 cm^{-1} and 1280 cm^{-1} (see Table 3). The band at 1432 cm^{-1} has been assigned to the C—O stretching mode of the η^2-acetaldehyde in previous studies in electrochemical [68] and UHV [78] environment. However, in the wavenumber range theoretically investigated, we did not observed the band corresponding to the C—O stretching mode of the η^2-acetaldehyde, and indeed, it should be quite weak in the SFG spectrum since the C—O bond should be nearly along the surface. In a general sense, the presence of η^2-acetaldehyde suggested by the three bands discussed above is in excellent agreement with an UHV study about the acetaldehyde adsorption on Rh(1 1 1) [72] and with some results previously reported by Davis and Barteau [78]. In an UHV study about the spectroscopic identification of intermediates in ethanol decomposition on Pd(1 1 1), Davis and Barteau [78] observed the η^2-acetaldehyde formation at 200 K. An additional interpretation for the band at 1432 cm^{-1} is to be associated with the C—O stretching mode of η^2-formaldehyde species. There is a good correlation between this band at 1432 cm^{-1} and that observed at 1420 cm^{-1} by Davis and

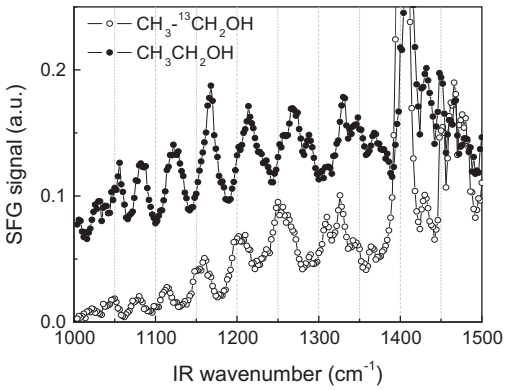

Fig. 9. SFG spectra (1000–1500 cm^{-1}) of the following interfaces: (0.1 mol L^{-1} CH_3CH_2OH + 0.5 mol L^{-1} $HClO_4$)/Pt (filled circles) and (0.1 mol L^{-1} CH_3—$^{13}CH_2$-OH + 0.5 mol L^{-1} $HClO_4$)/Pt (empty circles) at 0.05 V vs. RHE. The SFG peak at 1408 cm^{-1} and the SFG band at ~1475 cm^{-1} are not related to any molecular vibrational transition (see Section 3.1). The spectrum with regular ethanol has been displaced vertically for clarity of presentation.

Barteau [78] for methanol decomposition on Pd(1 1 1) under UHV conditions. In addition to the probable formation of η^2-acetaldehyde or η^2-formaldehyde, we cannot exclude the possibility of the presence of a η^2-acetyl species since the C—C stretching mode of a η^2-acetyl intermediate may be quite close to the C—O stretching mode of a η^2-acetaldehyde, at around 1430 cm^{-1}. Although evidence of formation of η^2-acetyl as an intermediate of the electro-oxidation of ethanol is lacking in the literature, it is very likely that the reaction pathway toward the CO and subsequent CO_2 formation may involve an adsorbed intermediate with both carbon atoms attached to the surface, which may be the precursor of these species. Therefore, based on our results, we tentatively propose that η^2-acetyl is an active adsorbed intermediate of the ethanol oxidation on Pt in acidic medium.

The bands at 1122 or 1168 cm^{-1} can also correspond to the C—C stretching mode of an ethylidyne-like adsorbate. In UHV, the C—C stretching mode of an ethylidyne adsorbed on Pt(1 1 1), from the ethylene decomposition, was characterized by a band at 1120 cm^{-1} [79]. Nevertheless, this mode assignment for adsorbed ethylidyne was based on a comparison with an ethylidyne tricobalt nonacarbonyl complex, as first outlined by Skinner et al. [80], that assigned a band at 1163 cm^{-1} to the C—C stretching mode of the ethylidyne. Therefore, we cannot exclude the possibility of any one of these bands (at 1122 or 1168 cm^{-1}) to be related with the C—C stretching mode of an ethylidyne-like adsorbate.

The band at 1736 cm^{-1} can be attributed to the C=O stretch of an adsorbed monodentate acetate species. This band assignment is in accord with that reported in an UHV study on the adsorption of acetic acid on Pd(1 1 1) [81] with the formation of monodentate acetate. In earlier investigations on the electrochemical oxidation of ethanol on Pt in acidic medium by conventional IR spectroscopy, the band at ~ 1740 cm^{-1} was attributed to the C=O stretching vibration of the carbonyl group of the acetaldehyde and acetic acid in solution [9,15,68]. However, this cannot be the origin of the band in the SFG spectroscopy, since it is not sensitive to molecules randomly oriented in solution.

Therefore, based on our experimental results in conjunction with our theoretical calculations and supporting information from the literature, we suggest for first time that η^2-acetaldehyde, η^2-acetyl, ethylidyne, and monodentate acetate can also be adsorbed intermediates of the ethanol electro-oxidation over platinum in acidic medium. All of these species contain two carbon atoms chain. In addition to them, we cannot ignore the possible formation of adsorbed intermediates containing only one carbon atom, which are also compatible with our SFG results and could be the precursors to C≡O formation.

The band at 1030 cm^{-1} matches the C—O stretching mode of a methoxy intermediate. This frequency is similar to that found for methoxy on Cu(1 1 0) [82], Ag(1 1 0) [83], and Pt(1 1 1) [84] surfaces in UHV studies.

We also suggest the formation of a $(Pt)_3$≡COH intermediate (COH residues) by considering the band at 1270 cm^{-1}, which can be attributed to its C—OH stretching mode, according to Iwasita and coworkers [85,86]. The band at 1214 cm^{-1} is close to the OH bending of a tertiary methanol derivative, $(Pt)_2$=CHOH, which was previously suggested for methanol oxidation on Pt in acidic medium, on the basis of a band at around 1200 cm^{-1} [85]. However, this peak does not shift significantly upon deuteration, so it cannot be an OH bending. Nevertheless, it may be assigned to the C—OH stretch of a tertiary methanol derivative, since its frequency is between those of COH residues (1270 cm^{-1}) and of the O—C—C stretching of tertiary ethanol derivative (1168 cm^{-1}).

Furthermore, as seen by the fact that the bands at 1736 cm^{-1} and 1330 cm^{-1} correspond to characteristic frequencies of the C=O stretching mode of modentate formate [87] and symmetric COO^- stretching mode of bidentate formate [88–90], we may also consider the possible formation of these species in the early stages of the ethanol oxidation on Pt.

Finally, the bands at 1370 cm^{-1} and 1496 cm^{-1} are compatible with the presence of residues like CH_3 and CH_2 directly attached to the Pt surface. These bands at 1370 cm^{-1} and 1496 cm^{-1} can be assigned to the CH_3 bending of Pt—CH_3 and CH_2 bending of $(Pt)_2$—CH_2, respectively.

Table 1 also summarizes the assignment of the vibrational bands and the identification of the reaction intermediates. Taken together, the bands at 1030 cm^{-1}, 1056 cm^{-1}, 1084 cm^{-1}, 1122 cm^{-1}, 1168 cm^{-1}, 1214 cm^{-1}, 1270 cm^{-1}, 1288 cm^{-1}, 1330 cm^{-1}, 1348 cm^{-1}, 1370 cm^{-1}, 1432 cm^{-1}, 1496 cm^{-1}, 1546 cm^{-1}, and 1736 cm^{-1} in SFG spectra and the predictions from the theoretical calculations confirm that ethoxy (1030 cm^{-1}, 1348 cm^{-1} and 1496 cm^{-1}), a secondary ethanol derivative – Pt—CHOH—CH_3 (1056 cm^{-1} and 1288 cm^{-1}) and acetyl species (1122 cm^{-1}, 1348 cm^{-1} and 1546 cm^{-1}), previously suggested at electrochemical environment based on ambiguous evidences, are active intermediates of the ethanol oxidation on Pt in acidic medium. In addition, some of these bands are also compatible with the presence of never before proposed two-carbon atoms intermediates, such as: η^2-acetaldehyde (1122 cm^{-1}, 1288 cm^{-1} and 1432 cm^{-1}), η^2-acetyl (1432 cm^{-1}), ethylidyne (1122 cm^{-1} or 1168 cm^{-1}), monodentate acetate (1736 cm^{-1}), and also 1-carbon atom intermediates, for instance: methoxy (1030 cm^{-1}), tertiary methanol derivative (1214 cm^{-1}), COH residue (1270 cm^{-1}), η^2-formaldehyde (1432 cm^{-1}), monodentate formate (1736 cm^{-1}), bidentate formate (1330 cm^{-1}), CH_3 (1370 cm^{-1}), and CH_2 (1496 cm^{-1}) residues. Moreover, we have confirmed the presence of intermediates previously documented with conventional IR spectroscopy: a tertiary ethanol derivative (1084 cm^{-1} and 1168 cm^{-1}), bidentate acetate (1330 cm^{-1}), and CO_{ad} (2056 cm^{-1}).

Based on the results discussed above, a simplified scheme of the electro-oxidation of ethanol on platinum in acidic solution is proposed in Fig. 10.

It is generally suggested that the ethoxy and the secondary ethanol derivative formation is the initial step of the mechanism of ethanol electro-oxidation on platinum. As mentioned by Iwasita and Pastor [17], the saturated alcohols have two active centers for adsorption on metal catalysts: the OH and the α-carbon (alcoholic carbon). Thus, the ethanol molecule would adsorb either through the oxygen atom or through the carbon atom after the rupture of either the O—H (1) or the C—H (2), respectively.

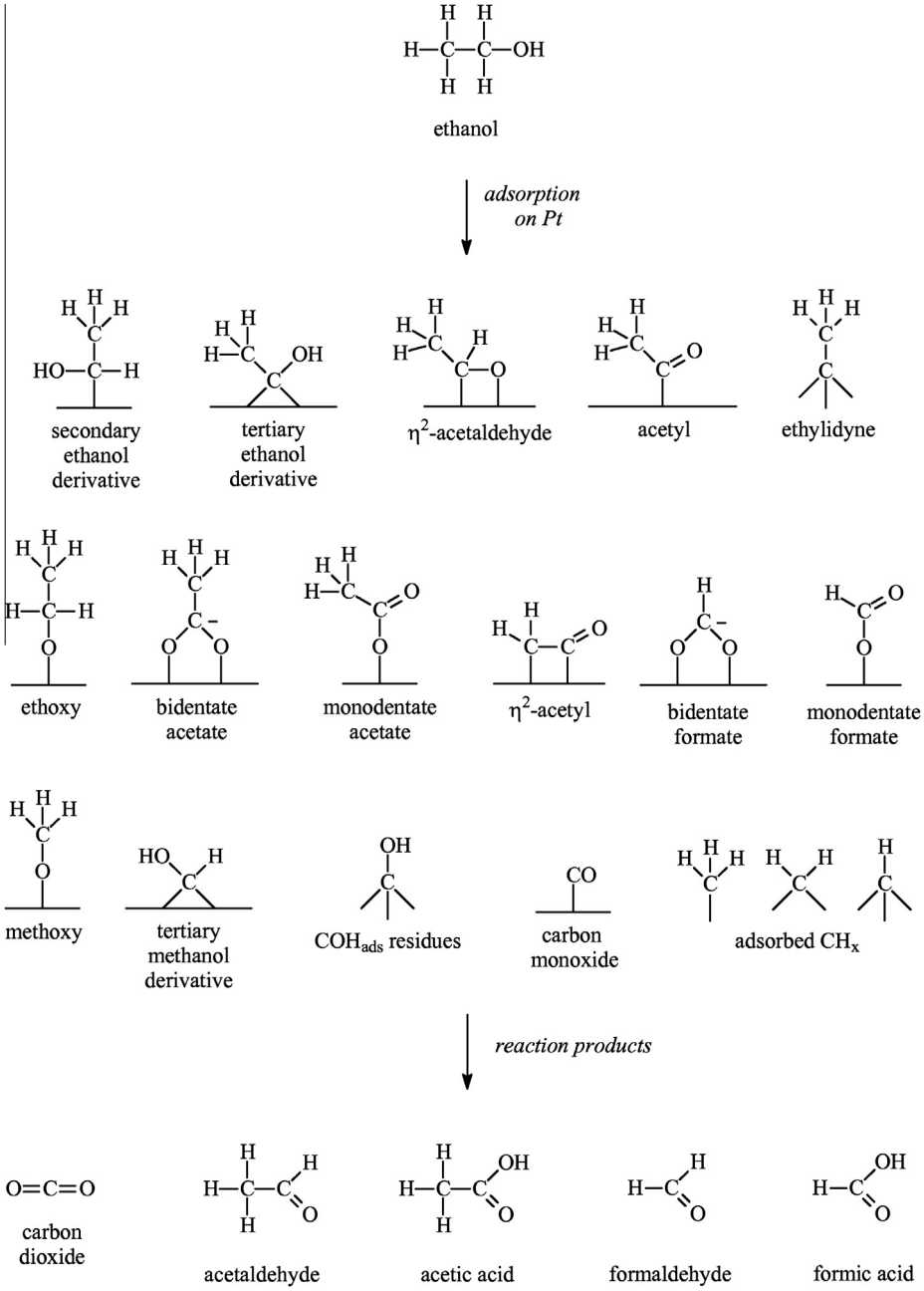

Fig. 10. Proposed intermediates of ethanol oxidation on platinum electrode in acidic medium. The geometry of the adsorbed intermediates is not considered in this scheme.

$$CH_3CH_2OH + Pt \rightarrow Pt - OCH_2CH_3(\text{ethoxy}) + H^+ + 1e^- \quad (2)$$

$$CH_3CH_2OH + Pt \rightarrow Pt - CHOHCH_3(\text{secondary ethanol derivative}) + H^+ + 1e^- \quad (3)$$

The presence of many other adsorbed intermediates, which should therefore be produced by the reaction of the species formed in (1) and (2), implies that the Pt surface is much more reactive than previously though. This coexistence of several adsorbates with comparable surface coverages (all detectable with SFG spectroscopy, whose signal is proportional to the square of the surface density) is in fact quite remarkable. It either means that all these adsorbates have very similar adsorption free energies, or the barrier for desorption is high enough so that the adsorbate coverage and diversity is governed by adsorption/reaction kinetics, and not by thermodynamic equilibrium. We believe the latter is more likely, since adsorption free energies should be quite sensitive to which atom bonds to Pt (C or O) and to the number of bonds per molecule (single-, double-, or triple-bonded to the surface).

In Fig. 10, additionally to the adsorbed intermediates of the ethanol oxidation on Pt in acidic medium, the well-known reaction products (CO_2, acetaldehyde, and acetic acid) and potential ones (formaldehyde and formic acid) are also represented. Based on our results, it is clear that the presence of complex adsorbed intermediates (with an intact C—C bond, and not only CO) up to the onset potential of the ethanol oxidation (0.5 V vs. RHE) should lead to partially oxidized products, such as acetaldehyde and acetic acid.

4. Conclusion

We have investigated the adsorbed intermediates of ethanol oxidation on platinum using SFG spectroscopy and DFT calculations. Generally, the effect of the applied potential on the reaction mechanism showed that in the pre-oxidation region (0.05–0.50 V), with increasing potential, the species formed at 0.05 V are partially converted to other adsorbed species, particularly to CO linearly bonded to the platinum surface. Also, we demonstrated that in the potential range between 0.50 V and 0.90 V, the adsorbed intermediates from ethanol oxidation are gradually oxidized with increasing potential and the free platinum sites are not re-occupied only by ethanol molecules, but also by other species. These species have strong interaction with the platinum surface and, as a result, they block the catalyst active area and inhibit the dynamic ethanol oxidation reaction (via adsorbed intermediates). We suggest that above 0.90 V, the ethanol adsorption and the C—C bond breaking are inhibited by the increasing presence of oxygenated species adsorbed on the platinum surface. In this manner, the adsorbed intermediates are weakly bonded and quickly transformed into partially oxidized products (with intact C—C bond) in such a way that the steady-state superficial concentration of the adsorbed molecules decreases below the detection limit of our apparatus.

The observed vibrational spectrum in the 1000–1400 cm^{-1} range is very complex, with at least 11 peaks (most of them assigned to C—O or C—C stretches), implying on the coexistence of several adsorbates, even at low potentials. It is at variance with those recently reported by Kutz et al. [34] for ethanol electro-oxidation on polycrystalline Pt, since they only detect adsorbed CO and acetate ions (and (bi)sulfate ions, for the case of sulfuric acid supporting electrolyte). We attribute this discrepancy to different surface preparation and SFG data acquisition methodologies: they clean the surface by electrochemical potential cycling and measure SFG spectra during a potential sweep using a 25 μm thick electrolyte layer, while we clean by H_2 flame annealing, adsorb ethanol from solution onto a pristine Pt surface held at low potentials and take the SFG spectra at fixed potentials with a window-electrode gap of 2–4 μm. It is interesting to note that although our cyclic voltammograms are similar to those in Ref. [34], the SFG spectra disagree, suggesting that voltammetry may not be as sensitive as SFG spectroscopy to ascertain surface quality and cleanliness.

Our theoretical methodology has satisfactorily supported experimental measurements and this mutual agreement provided additional insights concerning some of the adsorbed intermediates involved at electro-oxidation of ethanol. Our results show that ethoxy, secondary ethanol derivative and acetyl, previously suggested, but never before unambiguously documented, are active intermediates of ethanol oxidation in acidic medium. In addition, we report new spectroscopic evidences (in electrochemical environment) that are consistent with the presence of η^2-acetaldehyde, η^2-acetyl, ethylidyne, monodentate acetate, methoxy, tertiary methanol derivative, COH residues, η^2-formaldehyde, mono and bidentate formate, CH_3 and CH_2 residues. Moreover, the results obtained in this work confirm the presence of previously observed ethanol oxidation intermediates: tertiary ethanol derivative, bidentate acetate, and CO_{ad}.

Therefore, in addition to showing for first time that the reaction mechanism of the electro-oxidation of ethanol on Pt is much more complex than believed so far, we have also contributed for the understanding of the reaction mechanism by proposing new intermediates of the ethanol oxidation on Pt, among them some intermediates that have been previously proposed only in UHV environment and some intermediates that we propose here for the first time. This should stimulate both experimental and theoretical work to confirm the spectral assignments proposed herein and to elucidate the detailed reaction pathways for electro-oxidation of several organic molecules, especially at high potentials, where the low coverage prevented us from getting a vibrational spectrum of the interfacial species.

As a perspective for future work, we intend to investigate by SFG spectroscopy the adsorption and oxidation of ethanol at higher concentrations and temperatures (relevant to fuel cell operation) not only Pt-based catalysts, but also on other materials, such as Au and Pd, in acidic and alkaline media. This would contribute to the understanding of the influence of ethanol concentration, temperature, electrode material, and pH on the reaction mechanism.

Acknowledgments

We dedicate this manuscript to the memory of Prof. Francisco C. Nart. The authors gratefully acknowledge Professor Wolf Vielstich and Prof. Teresa Iwasita for the helpful discussions and guidance. We thank Hilton B. de Aguiar and L. Jay Deiner for assistance with experiments and discussions during the initial stages of this work. The authors also thank FINEP, CNPq, CAPES, and FAPESP for financial support of this work. M.F.S.P. and K.B. acknowledge CAPES/CNPq (process number PNPD0052086) and FAPESP (process number 05/02284-0) for postdoctoral fellowships, respectively.

References

[1] J.M. Leger, S. Rousseau, C. Coutanceau, F. Hahn, C. Lamy, Electrochim. Acta 50 (2005) 5118.
[2] C. Lamy, A. Lima, V. LeRhun, F. Delime, C. Coutanceau, J.M. Leger, J. Power Sources 105 (2002) 283.
[3] J. Goldemberg, Science 315 (2007) 808.
[4] E. Antolini, E.R. Gonzalez, Catal. Today 160 (2011) 28.
[5] D.M. dos Anjos, F. Hahn, J.M. Leger, K.B. Kokoh, G. Tremiliosi, J. Braz. Chem. Soc. 19 (2008) 795.
[6] J.F. Gomes, B. Busson, A. Tadjeddine, G. Tremiliosi, Electrochim. Acta 53 (2008) 6899.
[7] L. Jiang, A. Hsu, D. Chu, R. Chen, Int. J. Hydrogen Energy 35 (2010) 365.
[8] G.R. Salazar-Banda, K.I.B. Eguiluz, M.M.S. Pupo, H.B. Suffredini, M.L. Calegaro, L.A. Avaca, J. Electroanal. Chem. 668 (2012) 13.
[9] F. Vigier, C. Coutanceau, F. Hahn, E.M. Belgsir, C. Lamy, J. Electroanal. Chem. 563 (2004) 81.
[10] G.F. Cui, S.Q. Song, P.K. Shen, A. Kowal, C. Bianchini, J. Phys. Chem. C 113 (2009) 15639.
[11] C. Bianchini, P.K. Shen, Chem. Rev. 109 (2009) 4183.
[12] J. Willsau, J. Heitbaum, J. Electroanal. Chem. 194 (1985) 27.
[13] X.H. Xia, H.D. Liess, T. Iwasita, J. Electroanal. Chem. 437 (1997) 233.
[14] L.W.H. Leung, S.C. Chang, M.J. Weaver, J. Electroanal. Chem. 266 (1989) 317.
[15] T. Iwasita, B. Rasch, E. Cattaneo, W. Vielstich, Electrochim. Acta 34 (1989) 1073.
[16] B. Bittinscattaneo, S. Wilhelm, E. Cattaneo, H.W. Buschmann, W. Vielstich, Ber. Bunsen. Phys. Chem. 92 (1988) 1210.
[17] T. Iwasita, E. Pastor, Electrochim. Acta 39 (1994) 531.
[18] G. Socrates, Infrared and Raman Characteristic Group Frequencies, Wiley-Interscience, New York, 1980.
[19] B. Beden, M.C. Morin, F. Hahn, C. Lamy, J. Electroanal. Chem. 229 (1987) 353.
[20] R. Holze, J. Electroanal. Chem. 246 (1988) 449.
[21] J.W. Shin, W.J. Tornquist, C. Korzeniewski, C.S. Hoaglund, Surf. Sci. 364 (1996) 122.
[22] M. Heinen, Z. Jusys, R.J. Behm, J. Phys. Chem. C 114 (2010) 9850.
[23] P.B. Miranda, Y.R. Shen, J. Phys. Chem. B 103 (1999) 3292.
[24] Y.R. Shen, P. Natl, Acad. Sci. USA 93 (1996) 12104.
[25] S. Baldelli, N. Markovic, P. Ross, Y.R. Shen, G. Somorjai, J. Phys. Chem. B 103 (1999) 8920.
[26] S. Baldelli, J. Phys. Chem. B 109 (2005) 13049.
[27] M. Tadjeddine, J.P. Flament, A. Le Rille, A. Tadjeddine, Surf. Sci. 600 (2006) 2138.
[28] J.F. Gomes, B. Busson, A. Tadjeddine, J. Phys. Chem. B 110 (2006) 5508.
[29] K.A. Friedrich, W. Daum, C. Klunker, D. Knabben, U. Stimming, H. Ibach, Surf. Sci. 335 (1995) 315.
[30] C. Klunker, M. Balden, S. Lehwald, W. Daum, Surf. Sci. 360 (1996) 104.
[31] R.L. Behrens, A. Lagutchev, D.D. Dlott, A. Wieckowski, J. Electroanal. Chem. 649 (2010) 32.
[32] G.Q. Lu, A. Lagutchev, D.D. Dlott, A. Wieckowski, Surf. Sci. 585 (2005) 3.
[33] W.Q. Zheng, A. Tadjeddine, J. Chem. Phys. 119 (2003) 13096.
[34] R.B. Kutz, B. Braunschweig, P. Mukherjee, R.L. Behrens, D.D. Dlott, A. Wieckowski, J. Catal. 278 (2011) 181.

[35] B. Braunschweig, P. Mukherjee, R.B. Kutz, A. Wieckowski, D.D. Dlott, J. Chem. Phys. 133 (2010) 8.
[36] Y. Waseda, K. Hirata, M. Ohtani, High Temp. - High Press. 7 (1975) 221.
[37] W.R. Wadt, P.J. Hay, J. Chem. Phys. 82 (1985) 284.
[38] M.J. Frisch, G.W. Trucks, H.B. Schlegel, G.E. Scuseria, M.A. Robb, J.R. Cheeseman, J. Montgomery, J. A., T. Vreven, K.N. Kudin, J.C. Burant, J.M. Millam, S.S. Iyengar, J. Tomasi, V. Barone, B. Mennucci, M. Cossi, G. Scalmani, N. Rega, G.A. Petersson, H. Nakatsuji, M. Hada, M. Ehara, K. Toyota, R. Fukuda, J. Hasegawa, M. Ishida, T. Nakajima, Y. Honda, O. Kitao, H. Nakai, M. Klene, X. Li, J.E. Knox, H.P. Hratchian, J.B. Cross, V. Bakken, C. Adamo, J. Jaramillo, R. Gomperts, R.E. Stratmann, O. Yazyev, A.J. Austin, R. Cammi, C. Pomelli, J.W. Ochterski, P.Y. Ayala, K. Morokuma, G.A. Voth, P. Salvador, J.J. Dannenberg, V.G. Zakrzewski, S. Dapprich, A.D. Daniels, M.C. Strain, O. Farkas, D.K. Malick, A.D. Rabuck, K. Raghavachari, J.B. Foresman, J.V. Ortiz, Q. Cui, A.G. Baboul, S. Clifford, J. Cioslowski, B.B. Stefanov, G. Liu, A. Liashenko, P. Piskorz, I. Komaromi, R.L. Martin, D.J. Fox, T. Keith, M.A. Al-Laham, C.Y. Peng, A. Nanayakkara, M. Challacombe, P.M.W. Gill, B. Johnson, W. Chen, M.W. Wong, C. Gonzalez, J.A. Pople, GAUSSIAN 03, Revision-B.4, in, Gaussian, Wallingford., 2004.
[39] A.D. Becke, Phys. Rev. A 38 (1988) 3098.
[40] A.D. Becke, J. Chem. Phys. 98 (1993) 1372.
[41] A.D. Becke, J. Chem. Phys. 96 (1992) 2155.
[42] C.T. Lee, W.T. Yang, R.G. Parr, Phys. Rev. B 37 (1988) 785.
[43] E. Alonso, J.M. Casas, J. Fornies, C. Fortuno, A. Martin, A.G. Orpen, C.A. Tsipis, A.C. Tsipis, Organometallics 20 (2001) 5571.
[44] A. Bakalova, H. Varbanov, S. Stanchev, D. Ivanov, F. Jensen, Int. J. Quantum Chem. 109 (2009) 826.
[45] B. Giese, G.B. Deacon, J. Kuduk-Jaworska, D. McNaughton, Biopolymers 67 (2002) 294.
[46] Y. Zhang, L. Zhang, H.B. Tao, X.J. Sun, L.G. Zhu, Spectroc. Acta Pt. A-Molec. Biomolec. Spectr. 59 (2003) 493.
[47] M. Falk, P.A. Giguere, Can. J. Chem. 35 (1957) 1195.
[48] M. Okumura, L.I. Yeh, J.D. Myers, Y.T. Lee, J. Phys. Chem. 94 (1990) 3416.
[49] F. Dederichs, K.A. Friedrich, W. Daum, J. Phys. Chem. B 104 (2000) 6626.
[50] K.A. Friedrich, W. Daum, F. Dederichs, W. Akemann, Z. Phys, Chem. 217 (2003) 527.
[51] J.F. Gomes, K. Bergamaski, M.F.S. Pinto, P.B. Miranda, Optics Express, submitted for publication.
[52] A. Holmgren, L.M. Wu, W. Forsling, Spectroc. Acta Pt. A-Molec. Biomolec. Spectr. 50 (1994) 1857.
[53] D.K. Lambert, Solid State Commun. 51 (1984) 297.
[54] C. Korzeniewski, R.B. Shirts, S. Pons, J. Phys. Chem. 89 (1985) 2297.
[55] S. Holloway, J.K. Norskov, J. Electroanal. Chem. 161 (1984) 193.
[56] B.N.J. Persson, R. Ryberg, Phys. Rev. B 24 (1981) 6954.
[57] H. Wang, Z. Jusys, R.J. Behm, J. Phys. Chem. B 108 (2004) 19413.
[58] T. Iwasita, J. Braz. Chem. Soc. 13 (2002) 401.
[59] Y. Zhang, J. Zhao, G. Tang, L. Zhu, Spectrochim. Acta A 61 (2005) 697.
[60] B. Schrader, W. Meier, Raman/IR Atlas, Verlag Chemie, Weinheim, 1974.
[61] J.-P. Perchard, M.-L. Josien, J. Chim. Phys. 64 (1968) 1834.
[62] J.-P. Perchard, M.-L. Josien, J. Chim. Phys. 64 (1968) 1856.
[63] B.A. Sexton, Surf. Sci. 94 (1980) 435.
[64] B. Rasch, T. Iwasita, Electrochim. Acta 35 (1990) 989.
[65] L.W.H. Leung, M.J. Weaver, J. Phys. Chem. 92 (1988) 4019.
[66] R. Holze, W. Vielstich, Electrochim. Acta 33 (1988) 1629.
[67] A. Rodes, E. Pastor, T. Iwasita, J. Electroanal. Chem. 376 (1994) 109.
[68] M.H. Shao, R.R. Adzic, Electrochim. Acta 50 (2005) 2415.
[69] J.G. Chen, J.E. Crowell, J.T. Yates, Surf. Sci. 172 (1986) 733.
[70] B.A. Sexton, Chem. Phys. Lett. 65 (1979) 469.
[71] P. Uvdal, A.D. Mackerell, B.C. Wiegand, J. Electron Spectrosc. 64–5 (1993) 193.
[72] C.J. Houtman, M.A. Barteau, J. Catal. 130 (1991) 528.
[73] B.A. Sexton, Surf. Sci. 88 (1979) 299.
[74] D.A. Chen, C.M. Friend, Langmuir 14 (1998) 1451.
[75] S.C. Street, A.J. Gellman, J. Chem. Phys. 105 (1996) 7158.
[76] P. Uvdal, M.K. Weldon, C.M. Friend, Phys. Rev. B 50 (1994) 12258.
[77] J.L. Davis, M.A. Barteau, J. Am. Chem. Soc. 111 (1989) 1782.
[78] J.L. Davis, M.A. Barteau, Surf. Sci. 235 (1990) 235.
[79] R.G. Windham, B.E. Koel, J. Phys. Chem. 94 (1990) 1489.
[80] P. Skinner, M.W. Howard, I.A. Oxton, S.F.A. Kettle, D.B. Powell, N. Sheppard, J. Chem. Soc. Farad. T. II (77) (1981) 1203.
[81] R.D. Haley, M.S. Tikhov, R.M. Lambert, Catal. Lett. 76 (2001) 125.
[82] B.A. Sexton, A.E. Hughes, N.R. Avery, Surf. Sci. 155 (1985) 366.
[83] Q. Dai, A.J. Gellman, Surf. Sci. 257 (1991) 103.
[84] B.A. Sexton, Surf. Sci. 102 (1981) 271.
[85] T. Iwasita, F.C. Nart, J. Electroanal. Chem. 317 (1991) 291.
[86] T. Iwasita, F.C. Nart, B. Lopez, W. Vielstich, Electrochim. Acta 37 (1992) 2361.
[87] C. Xu, D.W. Goodman, J. Phys. Chem. 100 (1996) 1753.
[88] Y.X. Chen, A. Miki, S. Ye, H. Sakai, M. Osawa, J. Am. Chem. Soc. 125 (2003) 3680.
[89] M. Endo, T. Matsumoto, J. Kubota, K. Domen, C. Hirose, J. Phys. Chem. B 105 (2001) 1573.
[90] F.o. Hahn, B. Beden, C. Lamy, J. Electroanal. Chem. Interfacial Electrochem. 204 (1986) 315.
[91] T.H. Ellis, H. Wang, Langmuir 10 (1994) 4083.
[92] T. Kratochwil, M. Wittmann, J. Kuppers, J. Electron Spectrosc. 64–5 (1993) 609.
[93] N.s.r.d.n. NIST Computational Chemistry Comparison and Benchmark Database, Release 14, in: R.D. Johnson III, Ed., NIST, Gaithersberg, MD, 2006.